ISSN 2187-2260

Proceedings of the 25th Meeting of Japan CF Research Society

JCF 25

March 14-15, 2026

Vision Center Yokohama

Japan CF-Research Society

Edited by Shinya Narita

PREFACE

This is the proceedings of the 25th Meeting of the Japan CF-Research Society (JCF25), which was held at Vision Center Yokohama on March 14–15, 2026. Papers submitted to the editorial board have been peer-reviewed and revised for publication in these proceedings. Some papers were published as “A Note without Reviewing”.

For all meetings, from JCF1 through JCF25, we have published proceedings. For the meetings since JCF4, we have published electronic versions of the proceedings on our website in addition to printed versions. In view of the low efficiency and effectiveness of distributing information in printed form, we decided to discontinue the printed version beginning with JCF12. Only electronic versions have been published since then.

Finally, we would like to thank all the participants and everyone who contributed to organizing this meeting.

Editor-in-Chief
Shinya Narita, Iwate University
August 2026

CONTENTS

NOTE

高圧軽水素の多重パルス噴流衝突圧縮と CNZ 粒子による非化学的反応の探索研究

鈴木瑛介 [1]，内藤健 [1]，鈴木優太 [2]，馬場翔太郎 [2]，角拓磨 [2]，
内海政春 [3]，中田大将 [3]
[1] 早稲田大学，基幹理工学部，機械科学・航空宇宙学科
[2] 早稲田大学，理工学術院，基幹理工学研究科，機械科学・航空宇宙専攻
[3] 室蘭工業大学，航空宇宙機システム研究センター
E-mail: k-naito@waseda.jp

Abstract

In the field of condensed-phase nuclear reactions, excess heat has frequently been observed because of the interaction between metal particles and light hydrogen (H_2) (or deuterium (D_2)). We have conducted fundamental experiments using metal nano particles and H_2, and have confirmed that there is a positive correlation between injection pressure of supplied H_2 and temperature rise of metal nano particles, within a pressure range from atmospheric pressure to 8.1 MPa. In this paper, we developed a new reaction system which could generate high-temperature and high-pressure regions by focusing compression due to pulsed the super-multi-jets colliding. We conducted some experiments using metal nano particles and H_2 supplied at a maximum pressure of 14. 1 MPa with this new reaction system. In addition, we also estimated the heat generation and power output resulting from anomalous heat and compared them with past experimental results.

1. 研究背景

凝縮系核反応の分野では金属粒子と軽水素(H_2)および重水素(D_2)の接触による過剰熱が多く確認されている．A. Kitamura らによると ZrO_2 に粒子径 100 nm の Pd 粒子を分散させた試料に高圧の H_2 または D_2 を吸蔵させると再現性のある過剰熱 Anomalous large heat absorption が報告されている［1］．また，Y. Iwamura らによると Pd よりも安価な Cu を用いた CNZ(Cu-Ni-Zr 系合金)に H_2 を供給した際に PNZ(Pd-Ni-Zr 系合金)と同程度の Excess Heat が報告されている［2］．また，他研究機関の凝縮系核反応に関する研究では，主に 1 MPa 以下の H_2 を用いた実験で過剰熱は得られたと報告されている［3］．
一方，当研究室では多重衝突パルス噴流圧縮原理(図 1)を提唱してきた．この原理ではパル

ス状に生成した高速噴流群を一点で同時衝突させると，衝突点近傍にて高温・高圧縮領域を生成することが可能となる［4］．我々はこの原理を用いることで高温・高圧の H_2 を Pd, Cu，Ni などを中心とした金属粒子の触媒試料に供給して衝突させて，発熱反応を促進できると考えてきた [5].

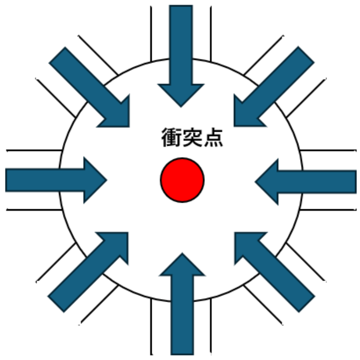

図 1　多重衝突パルス噴流圧縮原理

過去に，供給する H_2 の圧力と発熱量の関係性を調べるために，1 本の H_2 の噴流を金属試料に衝突させることができる反応容器を作成した．この反応容器では鏡像の原理から対向する 2 本の噴流の衝突を再現できる(図 2)．この反応容器を用いて実験を行いい，供給する H_2 の圧力が 1.0 MPa 以下の条件下で，供給する H_2 の圧力と温度上昇に正の相関が確認された［6].

さらに実験装置の耐圧性能を向上させることで供給する H_2 の圧力 8.1 MPa まで上昇させた実験を行ったところ，金属試料の温度上昇量が増加し，さらなる発熱を確認した［7] (図 3).

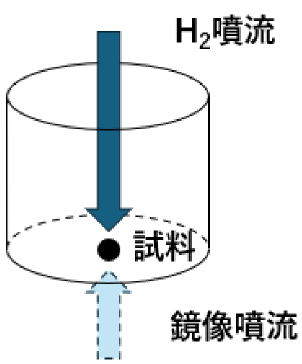

図 2　定容器型反応容器

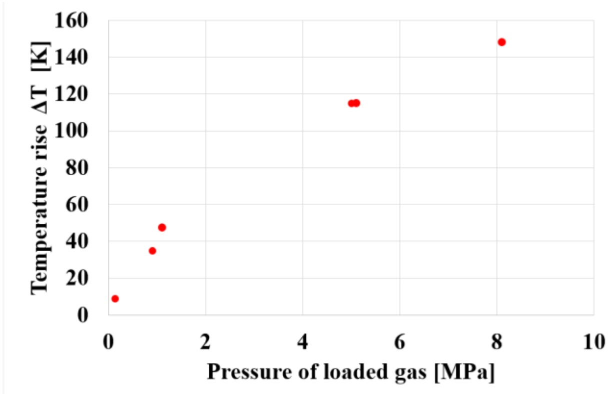

図 3　供給する H_2 の圧力と温度上昇量の関係

その後，多重衝突パルス噴流圧縮原理を応用した反応容器である多重衝突型反応容器を製作し，さらなる発熱量の向上を目指してきた(図 4)．多重衝突型反応容器は水素脆化に対して強いステンレス鋼(SUS316)で作られており，電磁弁から供給されるパルス噴流を平面で衝突させて生じるその高温・高圧の H_2 が試料に衝突することで反応の促進を狙っている．

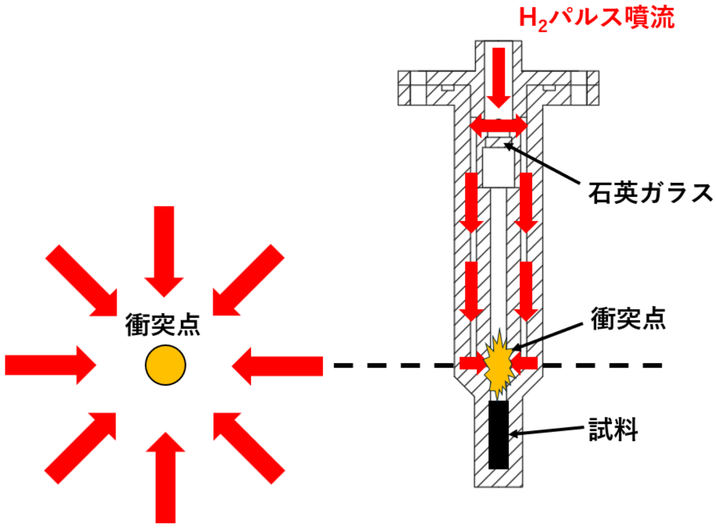

図 4　多重衝突型反応容器と H_2 の流路

そこで本研究では試料に供給する H_2 をさらに高圧化して発熱反応を促進してさらなる発熱量の増加を目指し，8.1 MPa 以上の圧力の H_2 を供給することで供給する H_2 の圧力と試料の温度上昇量の関係を計測し，発熱量および出力についても推定した．

2. 実験装置

本研究にて使用した実験装置概略図を図 5 に示す．本実験装置では多重衝突型反応容器を用いており，試料は反応容器底部に充填される．試料の温度は石英ガラスの観測窓を通して 2 色放射温度計(Sensortherm GmbH 社製，METIS-M322)を用いて計測している [8]．この 2 色放射温度計は非接触型の温度計で，試料から放出される赤外線のうち特定の 2 つの波長におけるエネルギー量の比率から温度を測定している．十分な保安距離を保った場所から遠隔でバルブを作動させる．また，試料が充填されている反応容器は外部にヒーターによって加熱させることができ，予め試料を設定した温度まで予熱できる．

まず，試料が舞わないように反応容器を真空ポンプで真空引きをする．反応容器内の圧力値が変動しなくなると真空引きは継続したまま反応容器外部のヒーターで設定した温度まで試料を予熱する．試料温度が試料温度まで達すると，真空引きを終了して水素ボンベ下流に位置するバルブを開けて H_2 のパルス噴流を供給する．試料温度の測定が終わると H_2 の

供給を終了して反応容器内部の H_2 を放出して窒素によるパージを実施する．

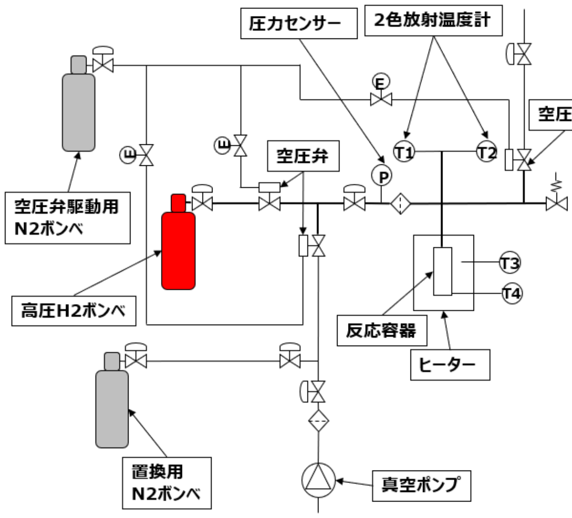

図 5　実験装置概略図

3. 実験概要

実験条件を表 1 に示す．本研究では Cu-Ni-Zr 系合金である CNZ の粉末 1.0 g を金属試料として用いる過去の実験結果との比較のために試料を予熱する温度は 573 K とした．供給する H_2 の圧力は圧力による比較のために 8.1 MPa と 14.1 MPa の 2 条件とした．また，反応容器に金属試料を入れずに H_2 を供給するブランク実験も行った．これは多重衝突パルス噴流圧縮原理による H_2 の断熱圧縮による発熱を除外するためである．測定する温度上昇量 ΔT は H_2 を供給する直前の試料温度から最大試料温度までの温度上昇量 $\Delta T_{apparent}$ からブランク試験での温度上昇量 ΔT_{blank} を引いた値とする．また，H_2 を供給してから試料が最大温度に到達するまでの時間を反応時間 Δt として測定した. サンプリング間隔は 1 msec とした．

表 1　実験条件

試料	CNZ（Cu-Ni-Zr 系合金）粉末
試料量	1.0 g
設定試料予熱温度	573 K
供給気体	H_2
供給気体圧力	8.1 MPa, 14.1 MPa

4. 実験結果

表 1 に示す実験条件の通り，CNZ の粉末 1.0 g に供給する H_2 の圧力が 8.1 MPa の条件での温度上昇量 $\Delta T_{apparent}$ の推移を図 6 に，供給する H_2 の圧力が 14.1 MPa の条件での温度上昇量 $\Delta T_{apparent}$ の推移を図 7 に示す. 0 sec でバルブを動作させて H_2 を反応容器に供給した. 温度上昇量 $\Delta T_{apparent}$ は供給する H_2 の圧力が 8.1 MPa の条件では 114.6 K，14.1 MPa の条件では 157.1 K となり，供給する H_2 の圧力を大きくした後者の 14.1 MPa の条件の方が大きい温度上昇量を得た．また，供給する H_2 の圧力が 8.1 MPa の条件では複数回の実験で同様の温度上昇量 ΔT を得て再現性を確認できた（付録参照).

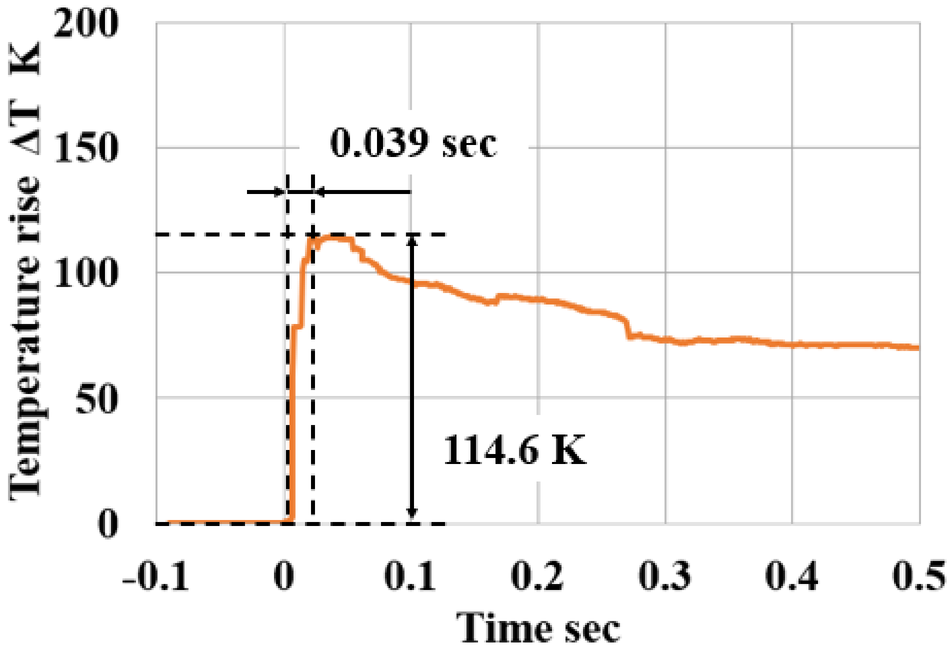

図 6　実験結果(CNZ 1.0 g，573 K，8.1 MPa)

なお, 反応容器に試料を入れずに H_2 を供給したブランク試験の温度上昇量 ΔT_{blank} の推移を図 8 に示す．8.1 MPa の H_2 を供給した条件では 7.6 K，12.1 MPa の H_2 を供給した条件では 13.2 K の温度上昇量 ΔT_{blank} を記録した.

8.1 MPa の条件では，ブランク試験における試料の温度上昇量 ΔT_{blank}(＝7.6 K)は、試料粉末に H_2 を供給した際の温度上昇量 $\Delta T_{apparent}$(＝114.6 K)より 1 桁程度以上小さいため，H_2 の高速噴流の衝突による流体加熱の影響は小さい.

14.1 MPa のブランク試験は行っていないが，8.1 MPa と 12.1 MPa の H_2 を供給した条件での温度上昇量 ΔT_{blank} から 14.1 MPa での温度上昇量 ΔT_{blank} を外挿して算出した. その結果，14.1 MPa の H_2 を供給した場合における流体加熱では 16.0 K 程度の温度上昇量 ΔT_{blank} と推

定された．なお、この流体加熱による温度上昇がゼロになるのは、大気圧レベルの場合と考えられる。これを含めた 3 つの圧力値（0.1 MPa、8.1 MPa、12.1 MPa）を横軸にとり、縦軸にブランク試験での温度上昇（0 K、7.6 K、13.2 K）をとって考えると、下に凸の曲線と考えられるため、実際には、16.0 K よりも大きい可能性がある。よって、14.1 MPa での流体加熱の影響度合いについては、今後、定量的な評価を行う必要がある。

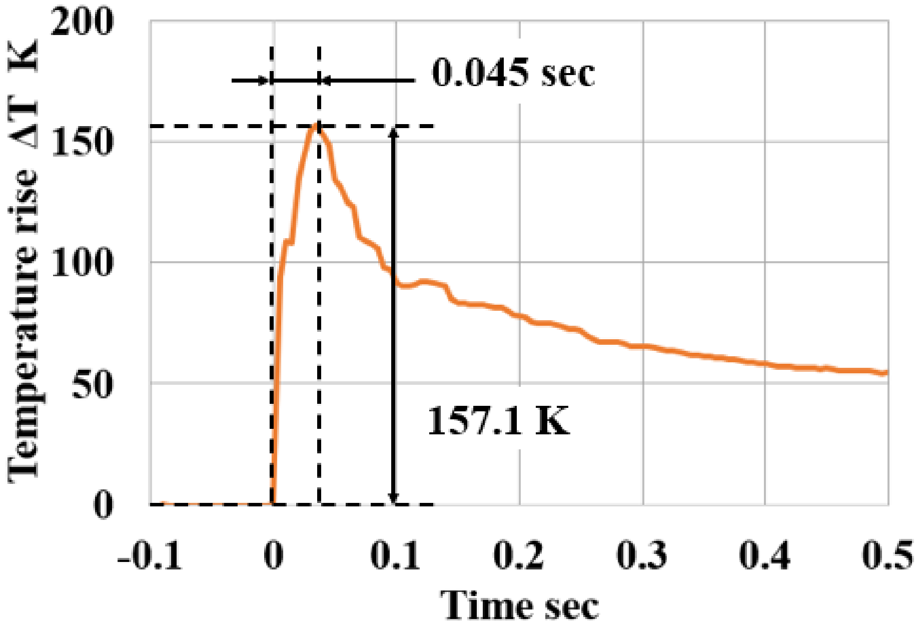

図 7　実験結果(CNZ 1.0 g，573 K，14.1 MPa)

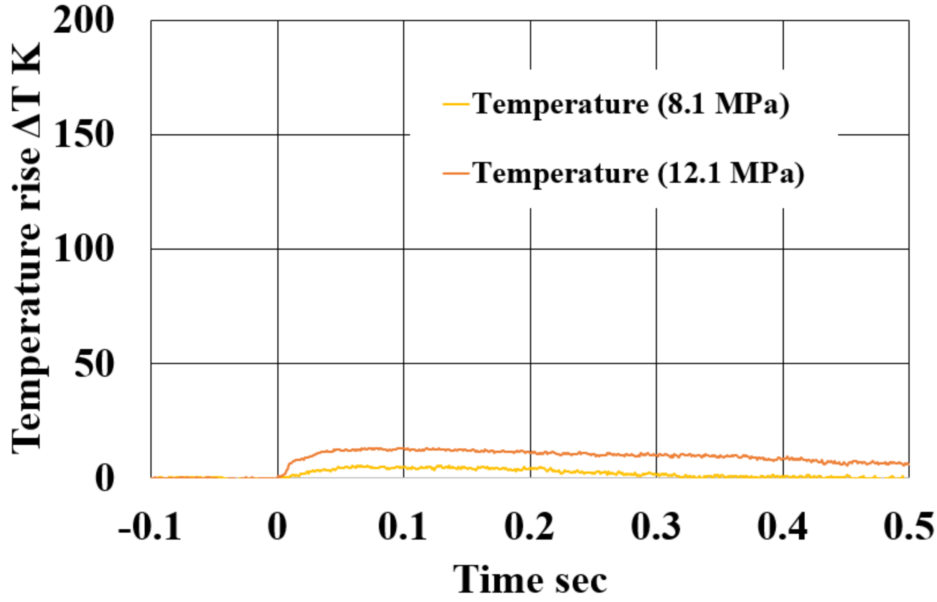

図 8　実験結果（試料無し，573 K, 8.1 MPa & 12.1 MPa）

5. 発熱量推定

実験結果から過剰熱の発熱量および出力の推定を行った．算出過程で以下の仮定を行った．

1. 実験で測定した温度上昇量ΔT は試料の発熱によって生じと仮定する．
2. 試料温度は実験中一定である．
3. 発生した熱量はすべて試料に吸収されたとする．

反応容器に残留している O_2 による試料金属の酸化や供給する H_2 による燃焼の化学反応による発熱量は総発熱量に比べて小さい［9］．また，CNZ に含まれる Cu の表面から 5 nm が酸化状態である［10］．これらの事実から酸化還元などの化学反応分は小さいとし，その他の熱のやり取りは考慮しない．上述したように、10 MPa 程度以下における高圧 H_2 の高速噴流の衝突圧縮によって発生する流体加熱はブランク試験の結果により評価した．また，反応容器金属壁からの熱伝達は考慮していないが, 熱が外部に逃げて温度低下させる効果であるため，実際の過剰熱の発熱量は推定した発熱量より大きいと考えられる．

発熱量および出力は以下の式(1)，(2)で定義する．

$$Q\ [\mathrm{J}] = \Delta T\ [\mathrm{K}] \times C_{sample}\ [\mathrm{J/K}] \quad (1)$$

$$P\ [\mathrm{W}] = Q\ [\mathrm{J}]/\Delta \mathrm{t}\ [\mathrm{sec}] \quad (2)$$

ここで，C_{sample}は試料の熱容量を表す．熱容量は比熱と質量の積で表現され，本実験で用いた CNZ の熱容量は$C_{sample} = 0.463$ [J/K]である．

表 2 に CNZ を用いた実験の発熱量および出力を示す. 発熱量および出力は温度上昇量ΔT と同じく供給した H_2 の圧力が大きい 14.1 MPa の条件で大きい結果を得た．

表 2　実験結果をもとに推定した発熱量

Sample	H_2 pressure	Temp. rise ΔT	Time Δt	Heat Generation	Heat output
CNZ	8.1 MPa	107.0 K	0.039 sec	49.5 J	1.27 kW/g
CNZ	14.1 MPa	141.1 K	0.045 sec	65.3 J	1.45 kW/g

また，過去に Pd-Ni-Zr 系合金である PNZ を用いて 8.1 MPa の H_2 を供給した実験の温度上昇量$\Delta T_{apparent}$の推移を図 9 に示す［11］．この実験では CNZ と同様の方法で発熱量および出力を推定したところ，発熱量は 231 J，出力は 0.0577 kW を記録した．比較のために出力を試料 1.0 g あたりに変換すると 0.0192 kW/g となり，本報告における CNZ を使用した場合（表２）は PNZ を使用した場合に比べて５０倍を超える大きい出力値を得た. なお、本論文の表２の結果は非接触の温度計、論文[10]の実験では熱電対を用いているが、温度上

昇ΔT はほぼ同じであった。また、本論文の反応容器(図 4)は、論文[10]の場合(図 2)に比べて、噴流群衝突圧縮度合をあげてあるが、その影響は 10 倍以下であったので、同じ計測条件では、PNZ に比べて CNZ の出力が大きいと考えている。ただし、発熱量および出力の値のばらつきもあるため、今後、詳細な検討が必要である.

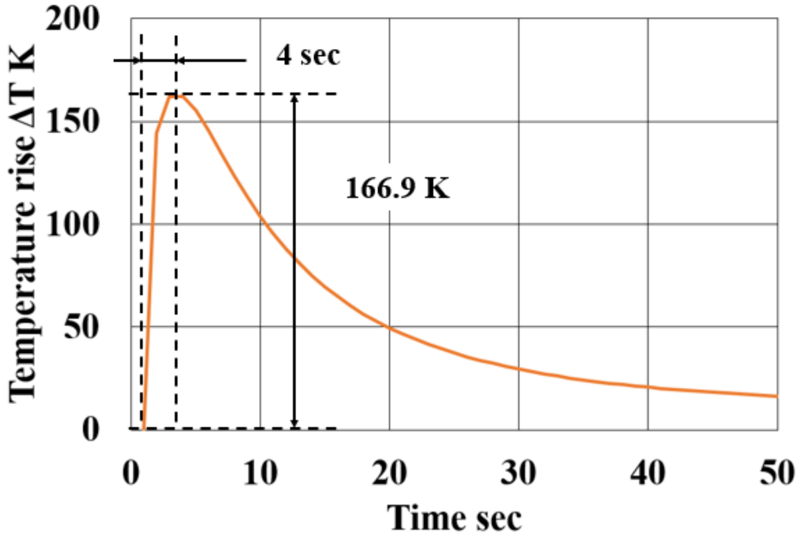

図 9　実験結果(PNZ 3.0 g，573 K，8.1 MPa) [11]

6. 結言

我々は多重衝突パルス噴流圧縮原理を用いて最大 14.1 MPa の高圧の H_2 を Cu-Ni-Zr 系合金の CNZ の粉末に供給する実験を実施した. 供給する H_2 の圧力が 8.1 MPa と 14.1 MPa の条件の場合を比較すると、より高圧の 14.1 MPa の条件での試料温度上昇量が大きい結果を得た. さらに，試料の温度上昇量から過剰熱の発熱量および出力を推定した結果，温度上昇量と同様に後者のより高圧の 14.1 MPa の条件で大きくなり，65.3 J，1.45 kW/g-CNZ であった．また，試料の単位質量あたりの発熱出力を過去の Pd-Ni-Zr 系合金の PNZ と比較したところ，CNZ を使用した場合は PNZ を使用した場合の出力を大きく上回った.

ただし、14.1 MPa での流体加熱の影響度合いについては、今後、定量的な評価を行う必要がある。

7. 付録

本論文（図 5）にて用いた実験装置には H_2 を供給するバルブ上流と高圧ボンベの間に拡大管路を設置している. これは一時的に H_2 を、より反応室近くにプールする役割をはたす.

バルブを開けて水素を供給する際、噴流群の衝突圧縮を向上させることにより反応容器内中央部圧力の上昇度合を高める役割を持つと考えて設置したものである．

なお，この拡大管路を設置する以前に、CNZ 粉末 1.0 g に 8.1 MPa の H_2 を供給する実験も実施した．その結果を図 10 と図 11 に示す．図 10、図 11 の結果はほぼ、同じレベルの温度上昇（発熱）を示し、図 6 の結果と同程度となっていることがわかる。(ただし、図 6 と比べてみると、バルブ上流と高圧タンクの間に設置した拡大管路の効果は実験誤差範囲と言える。)

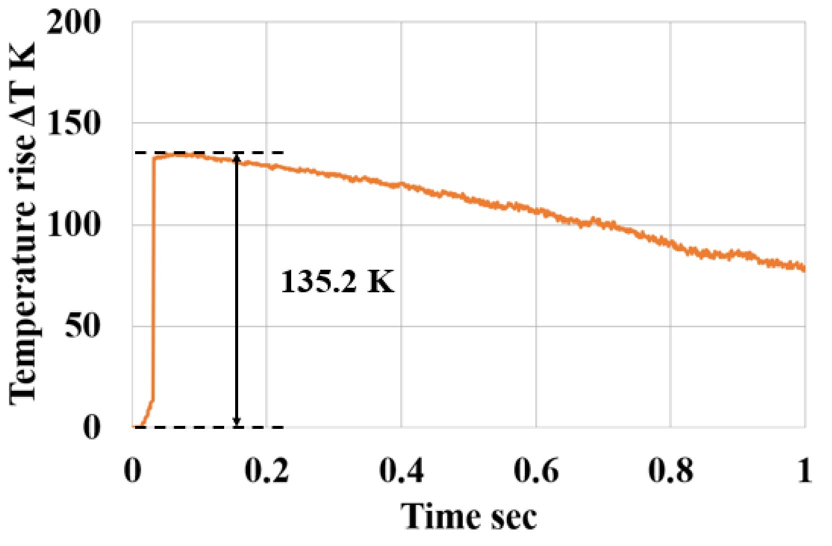

図 10　実験結果（CNZ 1.0 g，573 K，8.1 MPa，拡大管路無）

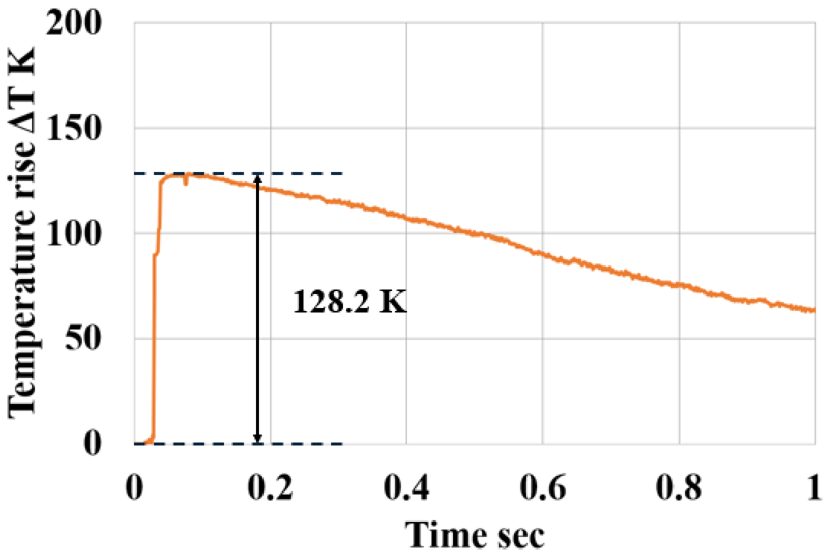

図 11　実験結果（CNZ 1.0 g，573 K，8.1 MPa，拡大管路無）

8. 謝辞

この研究は一般財団法人 熱・電気エネルギー技術財団(TEET)の助成を受けて実施されました．また，試料の CNZ をご提供いただいた株式会社テクノバに感謝申し上げます．本論文に関する実験は室蘭工業大学 航空宇宙機システムセンター 白老実験場にて実施しており，高野智之氏，学生の皆様にもご助言を賜り，実験の実施などにご協力いただきました．感謝申し上げます．

引用文献

[1] A. Kitamura, T. Nohmi, Y. Sasaki, A. Taniike, A. Takahashi, R. Seto and Y. Fujita, *Physics Letters A,* vol. 373, no. 35, pp. 3109-3112, 2009.

[2] Y. Iwamura, T. Itoh, J. Kasagi, and A. kitamura, "Anomalous Heat Generation Experiments Using Metal Nanoparticles and Hydrogen Gas," *Journal of Condensed Matter Nuclear Science,* vol. 29, pp. 119-128, 2019.

[3] NEDO,"金属水素間新規熱反応の現象解析と制御技術,"2017.

[4] K. Naitoh, "Engine". Int Patent 2010-133028, 27 Mar 2011.

[5] K. Naitoh, J. Tsuchiya, K. Ayukawa, S. Oyanagi, T. Kanase, K. Tsuru, R. Konagaya, "Fundamental experimental tests toward future cold fusion engine based on point-compression due to supermulti-jets colliding with pulse (fusine)," *Journal of Condensed Matter Nuclear Science,* 第 巻 24, pp. 236-243, 2017.

[6] T. Kobayashi, J. Shigemura, K. Naitoh, Y. Mori, R. Seto, and J. Hachisuka, "Temperature and Pressure Dependence of Anomalous Heat Generation Occurring in Hydrogen Gas Absorption by Metal Powder," *Journal of Condensed Matter Nuclear Science,* vol. 36, no. 1, pp. 318-326, 2022.

[7] T. Kobayashi, K. Naitoh, D. Okada, R. Nakagawa, Y. Toba, M. Uchiumi, D. Nakata, "Estimation of the Heat Generation of the Metal Composite Powder Absorbing the Pulsed Flow of Hydrogen Gas," *Journal of Condensed Matter Nuclear Science,* 第 巻 38, pp. 96-107, 2024.

[8] T. Kado, K. Naitoh, Y. Suzuki, S. Baba, Y. Toba, T. Kobayashi, M. Uchiumi, and D. Nakata, *Anomalous temperature increases in Cu nano particles exposed to colliding pulsed super-multi-jets of hydrogen gas,* Iwate: Abstract of ICCF26, 2025.

[9] Y. Iwamura, T. Itoh, S. Yamauchi, and T. Takahashi, "Anomalous heat generation that cannot be explained by known chemical reactions produced by nano-structured multilayer metal composites and hydrogen gas," *Japanese Journal of Applied Physics,*

第 巻 63, 2024.

[10] 鈴木茂, 一色実, “高純度金属における自然酸化膜の評価と制御,” *まてりあ,* 第 巻 37, 第 3, pp. 171-174, 1998.

[11] T. Kobayashi, K. Naitoh, D. Okada, R. Nakagawa, Y. Toba, M. Uchiumi, and D. Nakata, "Fundamental experiments of anomalous heat effect in metal composite powder exposed to pulsed high-pressure hydrogen gas," *Proceedings of the 23rd Meeting of Japan CF-Research Society (JCF23),* pp. 143-152, 2023.

The Cold Fusion Phenomenon in PdH_x and Detection of Tritium – A Historical Review of the Cold fusion Phenomenon (1) –

Hideo Kozima
Cold Fusion Research Laboratory
597-16, Yatsu, Aoi, Shizuoka, Japan 421-1202
Mail: hjrfq930@ybb.ne.jp, hjrfq930@gmail.com
Cold Fusion Research Laboratory Website: http://www.kozima-cfrl.com/

Key words;
Control experiment, cold fusion phenomenon, PdH_x, transition metal hydrides, tritium, super-diffusivity,

Abstract

The cold fusion phenomenon (CFP) was declared its existence in 1989 as caused by the presupposed $d - d$ fusion reactions in the PdD_x sample ($x \leq 1$). As an inevitable result of its premises, the PdH_x system was taken up as a natural system for the control experiment to the PdD_x experiment. In the several inappropriate premises assumed due to the presupposed $d - d$ fusion reactions, one of the most harmful assumptions was the PdH_x system only as the control experiment. Due to the observed excess energy in the PdH_x system, the experiments performed by a pioneering group lost credibility and devalued. Unfortunately, the premises of the $d - d$ fusion reactions as the cause of CFP was incorrect and therefore the results it implied were impossible to occur. In succeeding several years, there appeared a lot of experiments showing CFP in PdH_x systems and theoretical verification of the results was given using knowledge of quantum mechanics and complexity in the transition metal hydrides.

On the other hand, the tritium had been investigated from the beginning of CF research in relations to the presupposed mechanism of CFP. We noticed several problems raised by the presupposed inappropriate assumptions which hindered the progress of the scientific research of CFP very much. The detection of tritium revealed the properties of the nuclear reaction, the locality of its occurrence, which was later identified as a key characteristic that characterizes science of CFP.

This paper provides an overview of the history of PdH_x system research and tritium detection spanning over 35 years, illustrating a paradigm transition from conventional solid-state and nuclear physics to new solid-state-nuclear physics. We can give a correct interpretation for the important episodes in the whole program of the science of CFP now its full picture is beginning to be revealed.

1 Introduction

H. Poincaré once spoke about the foundations of science as follows [Poincaré 1902]: "*The man of science must work with method. Science is built up of facts, as a house is built of stones; but an accumulation of facts is no more a science than a heap of stones is a house. Most important of all, the man of science must exhibit foresight.*" [Poincaré 1902 (p. 141)]

This statement may seem to be stating an extremely obvious *truth*, but upon closer examination, one realizes that it contains extremely complex content. The problem lies in the fact that the man of science who choose facts lives in a paradigm of a normal science at that time.

Within the paradigm of a normal science, the strong rejection of new facts considered unconventional is evidence of the health of that science. This is described clearly by the historian of science T. Kuhn in his book *The Structure of Scientific Revolutions* as follows [Kuhn 1996]:

"By ensuring that the paradigm will not be too easily surrendered, resistance guarantees that scientists will not be lightly distracted and that the anomalies that lead to paradigm change will penetrate existing knowledge to the core." [Kuhn 1996 (p. 65)]

However, while it is understandable that the emergence of CFP was not easily accepted by scientists in pertinent sciences, it must be recognized that it also became a serious hindrance to scientific progress. Let's examine this problem from a historical perspective in this paper. Furthermore, I aim to highlight how we have to treat facts to construct a new scientific paradigm and offer some perspectives of the science of CFP.

2 CFP in PdH_x System

It is known in the nuclear physics that the nuclear reactions between two low-energy deuterons proceed in three ways:

$$d + d = 4He^* \rightarrow 3He\ (0.82\ MeV) + n\ (2.45\ MeV), \qquad (1)$$

$$\rightarrow t\ (1.01\ MeV) + p\ (3.02\ MeV), \qquad (2)$$

$$\rightarrow 4He\ (0.08\ MeV) + \gamma\ (23.77\ MeV), \qquad (3)$$

with branching ratios for these decay reactions $\approx 1 : 1 : 10^{-7}$.

M. Fleischmann and S. Pons [Fleischmann 1989] had expected occurrence of these reactions in their experiments with PdD_x ($x \leqq 1$) hoping realization of reactions between deuterons as known in nuclear physics [Kozima 2019]. They, however, did not obtain the result consistent with those given in Eqs. (1) – (3).

Dr. Fleischmann wrote later [Fleischmann 1991] as follows to reconcile their experimental results with the situation they had in front of them;

“An important key to the understanding of the system is given by the strange properties of D (and of H and T) in such lattices. We must ask: how can it be that D can exist at a ~100 molar concentration and high supersaturations without forming D_2 in the lattice? How can it be that D diffuses so rapidly through the lattice (diffusion coefficient > 10^{-7} cm^2 s^{-1} greater than that of either H or T!) whereas He is practically immobile?” [Fleischmann 1991 (p. 9)]

As the cold fusion research started with the premises of the *d* – *d* fusion reactions in the PdD_x system, people had taken the PdH_x system as the control system to check the occurrence of CFP in the PdD_x system. Unfortunately, this assumption has led to many misunderstandings in the development of experimental plan and also in the interpretation of experimental results.

3 Measurement of the Tritium

Nest, we take up the tritium as one of the important nuclear products such as neutron, proton, gamma, $^4_2$He and $^3_2$He investigated from the first stage [Kozima 1998 (Sec. 6.4)]. In my recent paper [Kozima 2026a], I investigated the social phase of tritium measurement which disturbed the progress of the research on CFP. In this section, we will focus on the role of tritium measurement in CFP.

In the nuclear products expected from the probable nuclear reactions in the cold fusion phenomenon, tritium and $^4_2$He are charged particles with fairly large masses. By this characteristic, they have strong interaction with particles in the system and could not be measured outside as born in the nuclear reactions. They have been measured in their stable states in the system giving not direct but indirect evidences of the reactions. Amounts of tritium and $^4_2$He give directly total numbers of events generating them in the experiment.

The experimental data sets on the tritium measurement had been discussed in our books and papers [Kozima 1998 (Sec. 6.4), 2006 (Sec. 2.6), 2026a]. Due to the +e charge of triton ($^3_1$H), the detection of tritium provided the first evidence of localized nuclear reactions at the CFP (see especially [Iyengar 1989, 1990, Srinivasan 1990a, 1990b, Mengoli 1991a, 1991b]).

We can see the localization of tritium in Fig. 3.1. In this figure, local tritium activity on a Ti target after a plasma focus shot in deuterium gas is shown by autoradiography at the electrode tip [Srinivasan 1990a].

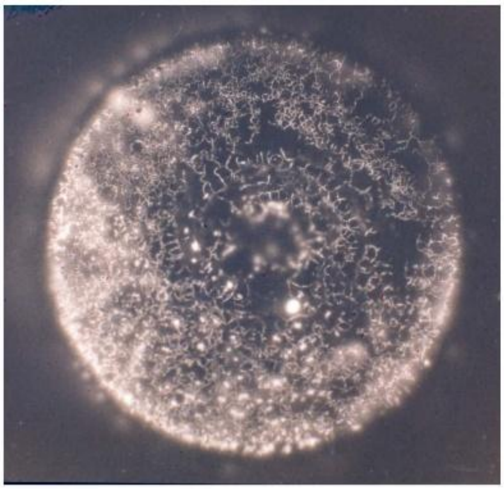

Fig. 3.1. Autoradiograph of central Ti electrode of PF device [Srinivasan 1990a (Fig. 2)].

Table 3.1. Tritium activity on titanium rod electrodes of PF device [Srinivasan 1990a (Table II)]

Electrodes	TA1	TA2	TA6
Date of PF Shots *	4^{th} Jan.	24^{th} May	4^{th} June
No. of Shots (+ ve)	50	25	-------
No. of Shots (- ve)	10	-------	25
Date of Measurement*	21^{st} Feb.	24^{th} May	4^{th} June
Counting Time (s)	300	300	300
Count Rate with Std. Source ‡ (cps)	6216	6290	11269
Count Rate with Electrodes (cps)	33.3	2.3	1.8
Background (cps)	1.2	1.6	1.5
Tritium Act. (MBq)	14.5±3.3	0.3±0.06	0.07±0.02

* All dates are in the year 1990.
‡ Standard source activity is (2800 ± 300) MBq.

We can cite a sentence reporting the localization of the tritium production from the paper by Srinivasan et al. [Srinivasan 1991b];
"One of the most interesting findings to emerge out of the autoradiographic imaging of deuterated Ti samples from different experiments is the fact that tritium is invariably concentrated in highly localized spots (fraction of a millimeter or less in size) each containing typically about 10^{12} to 10^{14} atoms (2 to 200 K Bq) of tritium." [Srinivasan 1990b (p. 1, italicized partially at citation)]

This feature of the local nature of nuclear reactions at the CFP was later confirmed by various experiments (cf. e.g., [Okamoto 1994, Bockris 1995, Iwamura 2006]) and provides an important clue to determining the nature of the CFP (see [Kozima 2009]).

Furthermore, we can see another characteristic of CFP, the *qualitative reproducibility*, in the experimental data sets of tritium generation using a simple radiographic method obtained by Srinivasan et al [Srinivasan 1990a]. The data shown in Table 3.1 show clearly the qualitative reproducibility of generation of tritium in the experiments of the plasma focus shot in deuterium gas.

The lack of quantitative reproducibility in CFP has been a point of criticism from opponents of the phenomenon from the beginning up to present. Now, we know that the cold fusion phenomenon is governed by complexity and it is the qualitative but not the quantitative reproducibility governing the events in CFP [Kozima 2006, 2013]. As we have seen in Table 3.1, the first clear evidence of the qualitative reproducibility was revealed by the experimental data by Srinivasan et al. [Srinivasan 1990a].

We have explained many events in CFP from formation of the optimum structures for the nuclear reactions to the inverse power relation of frequency vs. intensity ($1/f$ law in complexity) using the idea of complexity by now [Kozima 2013]. There was a clear tendency for unscientific discourse to run rampant due to misunderstandings regarding the difference between quantitative reproducibility in simple systems and qualitative reproducibility in complex systems regarding the reproducibility of measurement results.

The group that suffered the most damage was the Bockris7 research group at Texas A&M University, which had been working on tritium measurement from the beginning [Kozima 2026a]. At the 10th Anniversary of the announcement of the cold fusion phenomenon on 1999, Dr. J. O'M. Bockris wrote an essay "Cold Fusion 1999" at my request for the *CFRL News* published irregularly from Kozima's Cold Fusion Research Laboratory. Bockris' essay serves as a testament to the irrelevance of these accusations to true scientific inquiry.

4 Concluding Remarks on the New Paradigm emerging on the Cold Fusion Phenomenon

In this paper, we have given a brief discussion on the historical review of CFP focused on the PdH_x system and detection of tritium. In the former, we noticed difficulty to evaluate a fact in science and in the latter we found important finding of the qualitative reproducibility and localization of reactions in CFP.

For fairly long period, there had been many misunderstandings in both experimental planning and interpretation of results of the PdH_x system due to the discrepancy between the expected phenomenon and the actual reaction observed. The situation had gradually improved by the realization of the occurrence of CFP especially in NiH_x and Ni alloy systems. The experimental results in NiH_x system unintentionally obtained by J. Dash et al. [Dash 1994] and intentionally obtained by Ohmori et al. [Ohmori 2002, 2004] had been important data that marked a turning point in changing our perspective of CFP even if it did not attracted attention at that time and didn't become a subject of serious interest.

As the research of CFP progresses with the expansion of research fields e.g., to the super-diffusivity (SD) of hydrogen isotopes in transition metals, our point of view on CFP widened to include the extension of wavefunctions of occluded protons/deuterons and wavefunctions of nucleons in the lattice nuclei [Kozima 2009, 2013, 2026c]. The contradiction that was initially thought to be the case is now considered possible. The most notable example is that CFP was found to occur in the PdH system, which was initially thought to be a control system.

Thus, it turned out that what was initially thought to be an erroneous conclusion resulting from poor planning was in fact the disclosure of new facts. Perhaps we should say that in this case too, we were fortunate to encounter the mystery of science, which revealed the truth hidden behind the facts.

Anyway, we have to declare that the experiment in which S. Pons et al. performed to obtain the excess energy generation in the PdH_x system, supposed to be a control experiment at that time, was the first cold fusion experiment with PdH_x sample generated excess energy in the unintentional heating above perhaps 150 ºC by accident. The note "Warning! Ignition?" written on the events in Table 1.1 in the paper published in 1989 ([Fleischmann 1989 (Table 1)] may show something occurred in their laboratory, even if the details were hidden in the dark history destroyed by the accident! We will have to be taken their explanation in their paper [Fleischmann 1989 (p. 305)] very cautiously.

Perhaps, the experimental facts obtained in CFP together with those obtained in the super-diffusivity (SD) of H and D in transition metals, hydrogen electrode reaction (HER), and underpotential deposition (UPD) in transition metals show a new feature of solid state-nuclear physics closely related to the nuclear force interaction between nucleons in lattice nuclei and occluded protons/deuterons [Kozima 2023, 2026b, 2026c]. We can expect future developments of this science to a new paradigm between the solid-state physics and the nuclear physics along the line suggested in the above summary.

Acknowledgement

The author would like to express his gratitude to Dr. Jean-Paul Biberian who mediated my contact with Dr. Stanley Pons. Unfortunately, our communication was one-sided, but I think he understood the gist of the paper, and that alone made it worth contacting him through Dr. Biberian.

References

[Bockris 1995] J.O'M. Bockris and Z. Minevski, "Two Zones of 'Impurities' Observed after Prolonged Electrolysis of Deuterium on Palladium," Infinite Energy, 5 & 6, 67 – 70 (1995 – 96).

[Fleischmann 1989] M, Fleischmann, S. Pons and M. Hawkins, "Electrochemically induced Nuclear Fusion of Deuterium," J. Electroanal. Chem., 261, 301 – 308 (1989), ISSN: 1572-6657.

[Fleischmann 1991] M. Fleischmann, "Present Status of Research in Cold Fusion," Proc. ICCF2, Addition to the Conference Proceedings, pp. 475 – 487 (1991), ISBN 88-7794-045-X.

[Iwamura 2006] Y. Iwamura, T. Itoh, M. Sakano, N. Yamazaki, S. Kuribayashi, Y. Terada and T. Ishikawa, "Observation of Surface Distribution of Products by X-ray Fluorescence Spectrometry during D2 Gas Permeation through Pd Complexes" Proc. ICCF12 pp. 178 – 187 (2006).
[Iyengar 1989] P.K. Iyengar and M. Srinivasan ed., BARC STUDIES IN COLD FUSION (April - September 1989), BARC-1500, Library & Information Services, Bhabha Atomic Research Centre, Trombay, Bombay-400 085, December 1989.
[Iyengar 1990] P.K. Iyengar and M. Srinivasan, "Overview of BARC Studies on Cold Fusion," Proc. ICCF1 (Salt Lake City, Utah, USA, 1990), p. 62 (1990).
[Kozima 1998] H. Kozima, Discovery of the Cold Fusion Phenomenon – Development of Solid State-Nuclear Physics and the Energy Crisis in the 21st Century –, Ohtake Shuppan Inc., 1998, ISBN 4-87186-044-2.
[Kozima 2006] H. Kozima, The Science of the Cold Fusion Phenomenon, – In Search of the Physics and Chemistry behind Complex Experimental Data Sets –, 1st Edition, Elsevier, Amsterdam, 2006, ISBN-13: 978-0-08045-110-7.
[Kozima 2009] H. Kozima, "Non-localized Proton/Deuteron Wavefunctions and Neutron Bands in Transition-metal Hydrides/Deuterides," Proc. JCF9, pp. 84 – 93 (2009), ISSN 2187-2260.
[Kozima 2013] H. Kozima, "Cold Fusion Phenomenon in Open, Nonequilibrium, Multi-component Systems – Self-organization of Optimum Structure," Proc. JCF13 13-19, pp. 134 - 157 (2013), ISSN 2187-2260.
[Kozima 2019] H. Kozima, "On the 30th Anniversary of the Discovery of the Cold Fusion Phenomenon," Infinite Energy, 145 (May/June 2019), pp. 28 – 34 (2019), ISSN 1081-6372.
[Kozima 2023] H. Kozima, "Peculiarities of Physics and Chemistry in the Transition Metal Hydride," Journal of Condensed Matter Nuclear Science 37, pp. 98 - 110 (2023), ISSN 2227-3123.
[Kozima 2026a] H. Kozima, "In Search of Tritium – One of the Main Nuclear Products in the Cold Fusion Phenomenon in Solid State-Nuclear Physics –," J. Cond. Matter Nucl. Science, 41 (2026), ISSN 2227-3123 (to be published).
[Kozima 2026b] H. Kozima, M. Ohta and K. Kaki, "The Neutron; a Versatile, Talented and Wonderful Actor – A Historical Review of the Cold fusion Phenomenon (2) –," Proc. JCF25, 25-3 (2026), ISSN 2187-2260 (to be published).
[Kozima 2026c] H. Kozima, "Discovery of the Solid State-Nuclear Physics – A Historical Review of the Cold fusion Phenomenon (3) –," Proc. JCF25, 25-4 (2026), ISSN 2187-2260 (to be published).

[Kuhn 1996] T.S. Kuhn, The Structure of Scientific Revolution, The University of Chicago Press, Chicago and London, 1996, ISBN 0-226-45808-3 (3rd edition, 1996).
[Mallove 1991] E.F. Mallove, Fire from Ice – Searching for the Truth Behind the Cold fusion Furor –, John Wiley & Sons, Inc. New York, USA, 1991, ISBN 0-471-53139-1.
[Mengoli 1991a] G Mengoli, M. Fabrizio, C. Manduchi, G. Zannoni, L. Riccardi and A. Buffa, "Tritium and Neutron Emission in Conventional and Contact Glow Discharge Electrolyses of D2O at Pd and Ti Cathodes," Proc. ICCF2 (The Science of Cold Fusion), pp. 65 – 70 (1991), ISBN 88-7794-045-X.
[Mengoli 1991b] G Mengoli, M. Fabrizio, C. Manduchi, G. Zannoni, L. Riccardi, F. Veronesi and A. Buffa, "The Observation of Tritium in the Electrolyses of D2O at Palladium Sheet Cathodes," J. Electroanal. Chem. 304, pp. 279 – 2870 (1991), ISSN 1572-6657.
[Okamoto 1994] M. Okamoto, H. Ogawa, Y. Yoshinaga, T. Kusunoki and O. Odawara, "Behavior of Key Elements in Pd for the Solid State-Nuclear Phenomena Occurred in Heavy Water Electrolysis," Proc. ICCF4 (Hawaii, USA, Dec. 6 — 9, 1993), Vol.3, 14-1 – 14-8 (1994), TR-104188-V3 (EPRI, Palo Alto, California, USA).
[Ohmori 2002] Ohmori, S. Narita, H. Yamada, T. Mizuno and Y. Aoki, "Positive and Negative Energy Evolution and New Element Production in Critical Electrolysis with Palladium Electrode in K2CO3/H2O Solution," Proc. JCF4, pp. 22 – 26 (2002), ISSN 2187-2260.
[Ohmori 2004] T. Ohmori, T. Mizuno, H. Yamada and S. Narita, "Anomalous Isotopic Distribution of Palladium Generated during the Light Water Critical Electrolysis on Palladium Electrodes," Proc. JCF5, pp. 36 – 40 (2004), ISSN 2187-2260.
[Poincaré 1902] Henri Poincaré, Science and Hypothesis, p. 141 (1902). Translated by W.J.G., Dover Publications Inc. 1952. Library of Congress Catalog Card Number 53-13673.
[Srinivasan 1990a] M. Srinivasan, R.K. Rout, S.C. Misra, M. Lai, A. Shyam, P.S. Rao and P.K. Iyengar, "Observation of High Tritium Levels in Aged Deuterated Titanium Targets as Possible Evidence of Cold Fusion," Fusion Technol. 18, 88 (1990), ISSN 0748-1896.
[Srinivasan 1990b] M. Srinivasan, A. Shyam, T.C. Kaushik, R.K. Rout, L.V. Kulkarni et al., "Observation of Tritium in Gas/Plasma loaded Titanium Samples," AIP Conference Proceedings 228, pp. 1 – 21 (1990). Brigham Young Univ., Provo, UT: American Institute of Physics, New York.

Discovery of the Solid State-Nuclear Physics – A Historical Review of the Cold Fusion Phenomenon (3) –

Hideo Kozima
Cold Fusion Research Laboratory
597-16 Yatsu, Aoi, Shizuoka 421-1202, Japan
hjrfq930@ybb.ne.jp

Key words: solid state-nuclear physics, cold fusion phenomenon, nuclear force, neutron, super-nuclear interaction, superlattice, super-diffusivity,

Abstract

In this paper, we review the possible interaction of nucleons through the nuclear forces in materials where occur CFP and SD. To realize the interaction between nucleons due to nuclear forces in the relevant materials, we focused on the formation of superlattices of protons/deuterons and lattice nuclei through the self-organization known in nonlinear dynamics.

By expanding our research to include the presence of exotic nuclei within lattice nuclei, we demonstrated the potential to broaden our research field into the unknown territory of many-body nucleon systems, a subject that has been largely neglected in nuclear physics until recently.

The interaction between nucleons in CF materials by the nuclear forces gives to an end a new outlook to the super-nuclear interaction between neutrons in different lattice nuclei mediated by protons/deuterons occluded in the material. Furthermore, we can ultimately imagine a new perspective of the super-nuclear interaction between protons/deuterons occluded in the interstitial sites mediated by neutrons in lattice nuclei.

The super-nuclear interactions have opened the new world of the solid state-nuclear physics by the formation of neutron energy bands in the CF materials and the proton/deuteron energy bands in the materials where SD occurs, resulting in the cold fusion phenomenon in the former and the peculiarities of physical properties such as SD, HER and UPD in the latter. The CFP research results suggest the potential to contribute to cutting-edge research areas in nuclear physics, which are attracting attention in the study of neutron star matter and exotic nucleus.

1. Introduction

Since the announcement in 1989 of excess energy generation, a characteristic of the cold fusion phenomenon (CFP), in palladium deuterides, serious efforts have been made to explain the occurrence of nuclear reactions in solids (CF materials) without acceleration mechanisms, in a temperature range from near room temperature to several thousand degrees Celsius. In relation to the situation in CFP, we noticed other peculiarities such as the super-diffusivity (SD), the hydrogen electrode reaction (HER), and the underpotential deposition (UPD) observed in specific materials including the transition metal hydrides/deuterides and biotransmutation in biological organs investigated for more than a hundred years. We proposed that the interaction of nuclear forces between nucleons, known in nuclear physics, may be the common cause of the nuclear reactions in CFP, SD, and others.

It can be said that science is fundamentally an intellectual activity based on facts. After these more than 35 years since the announcement of the discovery of nuclear reactions in solids at around room temperature, named as the cold fusion phenomenon (CFP), I can't help but get the impression that our efforts to establish the science of CFP have been almost in vain. Despite earnest efforts to discover the truth hidden in the diverse experimental evidence showing nuclear reactions in CFP, we have yet to reach a unified understanding of this phenomenon, which must be seen as the evidence that CFP is a complex phenomenon that cannot be easily understood.

At this point, it may be necessary to look at the entire range of research conducted over this period that is not short from a historical perspective and consider how research in this field fits into modern society. We have inherited many lessons from the past. For example, how people reacted to facts that were revealed in ways we never expected, and how we can determine the direction of solid-state nuclear physics in the future. What we refer to here as *solid state-nuclear physics* is the science of the various nuclear reactions that occur due to the *nuclear force interaction* between nucleons in the pertinent solids. It has already been discussed [Kozima 2023] that solid state-nuclear physics includes not only CFP but also other wonderful phenomena observed in solids such as the super-diffusivity (SD), the hydrogen electrode reaction (HER), and the underpotential deposition (UPD). We investigate the situation more in detail in this paper from a new point of view including recent knowledge closely related to CFP obtained in the nuclear physics [Kozima 2026].

The phenomenological approach to CFP using the trapped neutron catalyzed fusion (TNCF) model with a single adjustable parameter n_n (the density of the *trapped neutron*) has given qualitative and sometimes semi-quantitative explanations for diverse experimental data sets including several observables (physical quantities) such as excess energy, transmuted nuclei, emitted neutrons and charged particles [Kozima 1998a, 2006a, 2026].

As the next step of the successful explanation of CFP using a phenomenological model [Kozima 1998a], we investigated the bases of the model using the quantum mechanical knowledge of solid-state physics and nuclear physics related to the atoms and atomic nuclei in the CF materials [Kozima 2004a, 2006a]. Perhaps it was a coincidence, but the opportunity to stay at PSU as a visiting professor at a time when I felt the need to study the quantum mechanical foundations of the model was a godsend.

The final answer to the validity of the assumptions presupposed in the TNCF model is summarized as (1) the self-organization of superlattices of the occluded protons/deuterons and lattice nuclei and (2) the super-nuclear interactions between neutrons in different lattice nuclei mediated by the occluded protons/deuterons. These two elements are discussed in detail in this paper.

It is shown that the non-local wavefunctions of the proton/deuteron in the transition metals are favorable for the concept of the neutron energy bands introduced to explain premises of the phenomenological models (TNCF and ND models).[Kozima 2009]

2.Self-organization of Superlattice of Host Elements and Occluded Protons/Deuterons

In the open and non-equilibrium dynamical system where energy and component materials are fed from outside, there appears patterns energetically unstable compared to the homogeneous structure without any structure. [Kozima 2013 (Sec. 3.3), 2016a (Sec. 3.8)].

In the case of the CFP, the optimum superlattice of the host lattice nuclei (e.g. Pd) and hydrogen isotopes (e.g. *d*) is apt to be formed in localized regions at surface layers with a width of about several microns where the number ratio $\eta = N_d/N_{\rm Pd}$ of the hydrogen isotope *d* and the host metal Pd is expected higher than other parts of the sample. Experimental data show that the formation of superlattice is possible when the ratio η becomes larger than ~ 0.8. The superlattice may be localized in small region with a diameter of about several micrometers as experimental facts show.

When the superlattice is formed at localized regions in the surface layer, it is possible to appear the neutron valence band by the super-nuclear interaction between neutrons in different lattice nuclei mediated by interstitial hydrogen isotopes [Kozima 2006a (Sec. 3.7.2)]

3. Nuclear Interactions of Lattice Nuclei and Occluded Hydrogen Isotopes in Transition Metal Hydrides

It had been determined that the hydrogen atom occluded in Pd *is completely ionized* as early as in 1936 by Mott and Jones [Mott 1936 (p. 200)]. Furthermore, we know by the recent experiment that the occluded protons/deuterons in *fcc* transition metals have nonlocalized wavefunctions which overlap to lattice nuclei [Kozima 2009]. Then, these protons/deuterons interact with uppermost neutrons in lattice nuclei through the nuclear force and finally the neutrons in different lattice nuclei interact each other through the *super-nuclear force* mediated by occluded protons/deuterons [Kozima 2013].

If we shift our focus from neutrons to protons, we see that the *super-nuclear interaction* mediated by neutrons in lattice nuclei occur between protons.

We have to accept the experimental facts that protons/deuterons occluded in *fcc* transition metals and alloys have nonlocalized wavefunctions especially in their excited states. In addition to this fact about the wavefunctions of occluded hydrogens/deuterons, there are experimental data that show extended-out wavefunctions of neutrons at the zero-energy level in such lattice nuclei as Pd and Ni of transition metals and C in graphite and biological CF-material [Kozima 2014b (Appendix A1)]. Furthermore, the recent investigation of the exotic nucleus had shown existence of neutron halo where loosely bound neutron wave functions are spatially extended , with diffuse , low density probability distributions [Casten 2000 (Sec. 11.2)].

Therefore, we can assume following situation where the wavefunctions of occluded protons/deuterons and the neutrons at the zero-level in the lattice nuclei or neutrons in the halo nuclei at lattice points overlap each other. The overlapping becomes larger and larger when the lattice nuclei become exotic and the number of neutrons N overwhelms the number of protons Z as we have discussed [Kozima 2008a] and also pointed out by nuclear physicist (e.g., Appendix A2 [Casten 2000 (pp. 428, 429)]. Then, there occurs an interaction between the occluded protons/deuterons and the neutrons in lattice nuclei in the CF materials through the nuclear force [Kozima 2004a, 2006a, 2009].

4. Super-nuclear Interactions between Neutrons in Different Lattice Nuclei and between Protons/Deuterons in Different Interstices

The interaction between a proton (deuteron) and a neutron in an adjacent lattice nucleus described above pulls two neutrons n_1 and n_2 in different lattice nuclei into coupling. We will call this coupling the "*super-nuclear interaction*" mediated by occluded (interstitial) protons (deuterons). [Kozima 2004a (Sec. 3), 2006a (Sec. 3.7.2), 2009 (Sec. 4)]

The essential points of the super-nuclear interaction mediated by occluded protons/deuterons are seen in the following procedure briefly cited from the book [Kozima 2004a (Sec. 3)];

"The overlapping of the proton wavefunction $\phi_p(R - b_j)$ on an interstice at b_j with a nucleon (neutron) wavefunction $\phi_n(x, a_i)$ on an adjacent lattice nucleus at a_i results in a proton-neutron interaction through the nuclear force. The nuclear interaction is expressed by a potential whose form is taken, for example, as the square-well type (neglecting spin-dependence and the imaginary part):

$V_s(r - R) = - V_0^{(s)}$, $(|r - R| < b)$

$=0$, $(|r - R| > b)$ (3.52)

where $V_0^{(s)} \sim 3.5$ MeV and $b \approx 2.2 \times 10^{-13}$ cm [Blatt and Weisskopf 1952]. The choice of this potential out of several possible types does not make a large difference to the result for the low energy phenomena we are considering in this book.

- - -

If there is an interaction between a neutron in a lattice nucleus and a proton/deuteron at an interstice b_j next to the lattice point a_i where the lattice nucleus is, there appears an interaction between two neutrons in two lattice nuclei at a_i and $a_{i'}$, interacting with the same proton/deuteron when $a_{i'}$ is also a neighbor of b_j. The coupled neutrons in lattice nuclei reveal a dispersed energy spectrum called the energy band as already explained generally in Section 3.5.2." [Kozima 2006a (pp. 102 – 103)]

It is easy extension of the *super-nuclear interaction between two neutrons* mediated by occluded protons/deuterons to the *super-nuclear interaction between two protons/deuterons* mediated by neutrons in lattice nuclei.

5. Neutron Energy Bands and Proton/Deuteron Energy Bands

It is easy to show that the super-nuclear interaction between two neutrons belonging to different lattice nuclei results in the formation of neutron bands [Kozima 2004a (Sec. 3), 2006a (Sec. 3.7.2.2)]. We can extend this idea of the neutron energy bands to the *proton/deuteron energy bands* formed by occluded protons/deuterons coupling with the super-nuclear interaction mediated by neutrons in lattice nuclei.

The neutrons in the neutron energy bands in CF materials can be treated as the neutrons in the neutron star matter (cf. e.g., [Baym 1971a, Negele 1973]), in the nuclear matter [Baym 1971b, Povh 2004] or in the nucleon many-body problem treated in the exotic nucleus (cf. e.g., [Casten 2000]). Similarly, the protons/deuterons in the proton/deuteron energy bands in SD materials as those participating in the super-diffusivity in transition metal hydrides/deuterides.

6. The Solid State-Nuclear Physics

As the history of science teaches us, a new science emerges when a new phenomenon is observed and found to be inexplicable by existing science. Thomas S. Kuhn developed his idea to explain the structure of scientific revolution using two concepts "paradigm" and "normal science" [Kuhn 1996].

We have discovered experimental facts in the interdisciplinary field between existing solid-state physics and nuclear physics that cannot be explained by previous knowledge, and are attempting to explain these phenomena using a new science named "solid-state-nuclear physics."

Although various attempts have been made, the current situation can be said to be as Kuhn describes it as follows:

"Probably the most striking of these is what I have previously called *the transition from the pre- to the post-paradigm period in the development of a scientific field*. - - - Before it occurs, a number of schools compete for the domination of a given field. Afterward, in the wake of some notable scientific achievement, *the number of schools is greatly reduced, ordinarily to one, and a more efficient mode of scientific practice begins*. The latter is generally *esoteric and oriented to puzzle-solving*, as the work of a group can be only when its members take the foundations of their field for granted." [Kuhn 1996 (p. 178)]. (Emphasis in italics added by the quoter).

We had presented a brief summary of the development of the solid state-nuclear physics [Kozima 2019] by the time the paper was written. We have now more data to put into our contemplation on a perspective of this field that is supported by broader and more detailed knowledge in nuclear physics.

We have given a brief survey of the present status of nuclear physics and solid state physics in relation of the present theme in the previous paper published in this Conference [Kozima 2026]. I plan to explain the details of the situation in another paper, but that paper will require a considerable number of pages.

7. Conclusion

This paper is the third and final of a series of papers presented at the 25th Annual Meeting of *the Japan CF-Research Society* (JCF25) entitled "*A Historical Review of Cold Fusion Phenomena*." We conceived of the *solid state-nuclear physics* (or rather the *solid state-nuclear science*) as a new science emerging halfway between solid-state physics and nuclear physics as a result of a paradigm-shifting scientific revolution. This is the result of research that combines experimental results obtained in the *solid state physics*, such as cold fusion phenomena (CFP), superdiffusivity (SD), hydrogen electrode reaction (HER), and underpotential deposition (UPD), with experimental results obtained in the *nuclear physics*, such as skin neutrons in the exotic nucleus and halo nuclei.

The TNCF model has been successful in understanding experimental data sets observed in complex and diverse CF materials consistently, which has led to the need for a theoretical explanation for the validity of the model. Especially demanded is the possible participation of neutrons in the formation of the neutron energy bands and the explanation of nuclear reactions generating nuclei with large changes of the proton number Z and the neutron number N (= $A - Z$) from those of the nuclei pre-existed in the CF materials. This problem had been successfully investigated in the second paper presented in this Conference [Kozima 2026]. The development in the nuclear physics in the terra incognita of the exotic nucleus suggested the value of research in this field. We can expect a development this terra incognita by inclusion of CFP in the nuclear physics of the exotic nucleus.

The recognition of the super-nuclear interaction in the transition metal hydrides/deuterides suggested by CFP had given a hint to solve problems left unsolved in the physics and chemistry of transition metal hydrides/deuterides such as super-diffusivity (SD), the hydrogen electrode reaction (HER) and the underpotential deposition (UPD). These problems together with CFP are the main themes of the solid state-nuclear physics we can consider at present. We hope that prospects on this problem given in this and the preceding papers will arouse interest in research and provide clues to solutions in these areas.

Due to space limitations, the explanation of the solid state-nuclear physics is incomplete.

8. References

[Baym 1971a] G. Baym, H.A. Bethe and C.J. Pethick, "Neutron Star Matter," *Nuclear Physics*, **A175**, pp. 225 – 271 (1971), ISSN 0375-9474.

[Baym 1971b] G. Baym, C. J. Pethick and P. G. Sutherland, "The Ground State of Matter at High Densities: Equation of State and Stellar Models," *Astrophys. J.* **170**, pp. 299 – 317 (1971), ISSN 0004-637X.

[Casten 2000] R.F. Casten, *Nuclear Structure from a Simple Perspective,* 2nd Edition, Oxford University Press, 2000, ISBN 0-19-850724-0.

[Kozima 1998a] H. Kozima, *Discovery of the Cold Fusion Phenomenon – Development of Solid State-Nuclear Physics and the Energy Crisis in the 21st Century –*, Ohtake Shuppan Inc., 1998, ISBN 4-87186-044-2. The "References" in this book is posted at the CFRL (Cold Fusion Research Laboratory) Website:

http://www.kozima-cfrl.com/Books/bookse/bookse.html

[Kozima 2004a] H. Kozima, *Quantum Physics of Cold Fusion Phenomenon,* Nova Science Publishers, Inc., New York, 2004, ISBN 1-59454-003-9.
[Kozima 2006a] H. Kozima, *The Science of the Cold Fusion Phenomenon*, *– In Search of the Physics and Chemistry behind Complex Experimental Data Sets –*, 1st Edition, Elsevier, Amsterdam, 2006, ISBN-13: 978-0-08045-110-7, ISBN-10: 0-080-45110-1.
[Kozima 2008a] H. Kozima, "Physics of the Cold Fusion Phenomenon," *Proc. ICCF13,* pp. 690 – 703 (2008), ISBN 978-5-93271-428-7.
[Kozima 2009] H. Kozima, "Non-localized Proton/Deuteron Wavefunctions and Neutron Bands in Transition-metal Hydrides/Deuterides," *Proc. JCF9*, pp. 84 – 93 (2009), ISSN 2187-2260.
[Kozima 2013] H. Kozima, "Cold Fusion Phenomenon in Open, Nonequilibrium, Multi-component Systems – Self-organization of Optimum Structure," *Proc. JCF13* **13-19**, pp. 134 - 157 (2013), ISSN 2187-2260.
[Kozima 2014b] H. Kozima, "The Cold Fusion Phenomenon – What is It?" *Proc. JCF14:* 14-16, pp. 203 – 230 (2014), ISSN 2187-2260.
[Kozima 2016a] H. Kozima, "From the History of CF Research – A Review of the Typical Papers on the Cold Fusion Phenomenon –," *Proc. JCF16,* **16-13,** pp. 116‐157 (2016), ISSN 2187-2260.
[Kozima 2019] H. Kozima, "Development of the Solid State-Nuclear Physics," *Proc. JCF19,* **19-15**, pp. 112 – 147 (2019), ISSN 2187-2260.
[Kozima 2023] H. Kozima, "Peculiarities of Physics and Chemistry in the Transition Metal Hydrides" *Journal of Condensed Matter Nuclear Science* **37**, pp. 98 - 110 (2023), ISSN 2227-3123.
[Kozima 2026] H. Kozima, M. Ohta and K. Kaki, "The Neutron; a Versatile, Talented and Wonderful Actor – A Historical Review of the Cold fusion Phenomenon (2) –," *Proc. JCF25*, **25-3**, pp. (2026), ISSN 2187-2260 (to be published).
[Kuhn 1996] T.S. Kuhn, *The Structure of Scientific Revolution*, 3rd edition, The University of Chicago Press, Chicago and London, 1996, ISBN 0-226-45808-3.
[Mott 1936] N.F. Mott and H. Jones, *The Theory of the Properties of Metals and Alloys*, Dover Publications, Inc., New York, 1958, Library of Congress Catalog Card Number: 58-11279.
[Negele 1973] J.W. Negele and D. Vautherin, "Neutron Star Matter at Sub-nuclear Densities," *Nuclear Physics*, **A207**, pp. 298 - 320 (1973) , ISSN 0375-9474.
[Povh 2004] B. Povh, K. Rith, C. Scholz and F. Zetsche, *Particles and Nuclei*, 4th Edition, Springer-Verlag, Berlin, 2004, ISBN 3-540-20168-8.

The Neutron; a Versatile, Talented and Wonderful Actor in Physics – A Historical Review of the Cold fusion Phenomenon (2) –

H. Kozima, M. Ohta* and K. Kaki**
Cold Fusion Research Laboratory
597-16 Yatsu, Aoi, Shizuoka 421-1202, Japan
*Correspondence author; mohta@air.ocn.ne.jp
**Faculty of Science, Shizuoka University
836 Oya, Suruga, Shizuoka 422-8529, Japan

Key words;
Cold fusion phenomenon, neutron, tritium, trapped neutron catalyzed fusion

Abstract

Since the discovery of nuclear reactions in solids at near room temperature, researchers in the field of cold fusion phenomenon (CFP) have paid careful attention to neutrons, which are thought to be closely related to nuclear reactions that occur in solids for which no acceleration mechanism can be considered. The neutron has been an important particle in nuclear physics since its discovery in 1932. The history of nuclear physics shows that its new developments have been made as the properties of neutrons had been elucidated through experiments. Needless to say, this is also the basic principle that should be followed in research at CFP. Focusing on this point, we provide a brief history of the development of nuclear physics with the elucidation of the nature of the neutron and an overview of the history of CFP in relation with neutrons.

1. Introduction

Human intellectual activity, especially scientific activity, can be seen to have three phases (faces); *experimental*, *theoretical* and *applicational phases (faces)*.

Many would agree that the natural sciences made remarkable progress in the 17th century, and that the most spectacular achievements were made in Britain. A Japanese science-historian H. Nakajima has focused on this fact and has discussed the rise and fall of *the theoretical and the experimental sciences*, the two main trends in physics at the time [Nakajima 1996]. He has used his method in his analysis of the achievements of two representative physicists of this era, Robert Hooke and Isaac Newton, as his subject.

To modernize his classification, we can add a third science, *the applied science* or the *applicational science*, corresponding to the applicational face of the above classification. In the consideration of the historical review of the cold fusion phenomenon (CFP) in relation to the elucidation of the nature of neutrons contemplated in this paper, we use the Dr. Nakajima's point of view adding a third science, the applicational science.

2. The Neutron in a Nucleus

The neutron is discovered by J. Chadwick in 1932 [Kozima 2006 (Topic 6)]. Since their discovery, neutrons have always played a central role in nuclear physics. It is necessary, however, to consider the great role that neutrons have played in the development of nuclear physics from a methodological point of view. Without fear of being misunderstood, it can be said that the main research method in nuclear physics, including the use of neutrons, is a *phenomenology*.

Neutrons, as elementary particles, have both particle and wave properties, and free neutrons undergo beta decay with a half-life of 886.7 s. After the discovery of the neutron, atomic nuclei are thought to be made up of neutrons and protons. The protons and neutrons are apparently the most permanent components of nuclear matter even if they are inseparable in that they can be converted into each other, and are therefore called *nucleons*.

The neutrons within atomic nuclei have the following properties: Nucleons (protons and neutrons in a nucleus) are hold together by constant exchange of pions between the nucleons. Pions are elementary particles that interact with neutrons and protons. Pions have about one-sixth the mass of a proton and come in three varieties: positively charged, negatively charged, and uncharged.

The evolution of the nuclear picture in response to accumulated experimental evidence has been explained in every textbook (e.g. [Jelley 1990]). Recently, the use of the new technique of RNBs *(radioactive nuclear beams)* revealed profound world of the exotic nucleus (cf. e.g. [Casten 2000]) in the unknown regions far out of known nuclei.

Even if there are extensive investigations on the nature of the neutron since its discovery in 1932, there remain inexplicable questions obtained in experiments about the nature of the neutron. Elementary particle physicists are struggling with them to construct a theory to reconcile the experimental facts as a nuclear scientist give a brief summary [Alexandrov 1992 (p. 15)].

3. The Neutron as Waves in Solids

As a quantum mechanical entity, the neutron naturally possesses both particle and wave properties. It is explained briefly as follows [Alexandrov 1992]:

"Before discussing the particle properties of the neutron, a consideration of the general question of the wave properties of the neutron seems justified. We outline here the wave properties of neutrons which are used as the basis for many experiments on the study of their fundamental properties.

It is well known that under certain conditions the behaviour of a particle is wave-like. Then a wavelength λ *given by the de Broglie relation*

$$\lambda = h/p \qquad (1.1)$$

is associated with the particle, where p is the particle momentum. Wave phenomena, in particular interference effects, are observed whenever the wavelength is comparable in order of magnitude with the size of an object inserted in the beam. The wavelength of thermal radiation (E = 0.025 eV) is 0.18 nm, so one may expect an X-ray-like diffraction from a crystal. The construction of nuclear reactors made available high fluxes of thermal neutrons that paved the way for the development of a new branch of nuclear physics – neutron optics. Principal neutron optical phenomena are well described in terms of the so-called kinematical theory of diffraction that neglects the interaction between the transmitted and reflected waves. Modern neutron optics is based the dynamical diffraction theory. At the beginning of this century Darwin and Ewald in their work devoted to X-ray radiation laid the foundation of the theory which takes into account the interaction of the transmitted radiation with the reflected radiation. Now the dynamical diffraction theory has been successfully extended to neutron radiation (see, for example, [Ref. 1]). This diffraction pattern calculated in terms of the dynamical theory looks virtually the same as that given by the kinematical theory, but with intensities which may differ by more than a factor of 10. The dynamical theory has predicted some phenomena for which there was no place in the kinematical theory; all of them have been confirmed experimentally (fine fringe structure observed in the experiments on neutron scattering by perfect crystals, pendelloesung effect, neutron interferometry, etc.).

[Ref. 1]. Dachs, H. (ed.) (1978).*Topics in current physics: Neutron diffraction*. Springer, Berlin." [Alexandrov 1992 (pp. 1 – 2)]

It should be remembered that astute nuclear physicists have focused on the role that neutrons play in the realm of low-energy nuclear physics [Kozima 2016a (Sec. 3.9)]. They have worked with neutrons to investigate characteristics of neutrons (e.g., [Tervisidis 1990, Steyerl 2020, Singh 2025]) and structures of materials (e.g., [Shull 1956, Molina 2021, 2023, Pavan 2025]) using high density neutron flux supplied by nuclear reactors (e.g., [Richtmyer 1976 (Sec. 25.21)]

4. The Neutron and the Cold Fusion Phenomenon (CFP)

In 1989, preliminary experimental results were published by Fleischmann et al. [Fleischmann 1989] showing that nuclear reactions may occur in solids at temperatures close to room temperature. This phenomenon is called the *cold fusion phenomenon* (CFP) due to the reason explained in Kozima's paper [Kozima 2019] published at the 30th anniversary of their paper:

"*We notice that the words "Cold Fusion" and "Cold Fusion Phenomena" are used in the titles of several Fleischmann's papers. In the words "Cold Fusion" he had given a special meaning as we see in Section II where we survey his mental process resulted in the discovery of the CFP."* [Kozima 2019].

Therefore, we would like to use the term *Cold Fusion Phenomenon* (*CFP*) to refer to "the nuclear reactions and accompanying events occurring in a non-equilibrium, open system (with external particle and energy inputs) consisting of solids containing high density hydrogen isotopes (H and/or D) in ambient radiation" belonging to the Solid State-Nuclear Physics (SSNP).

To gain a comprehensive understanding of CFP, we constructed a phenomenological model (TNCF model) that assumes the existence of metastable thermal neutrons (trapped neutrons) in CF material, and succeeded in qualitatively, and sometimes quasi-quantitatively, explaining many experimental facts [Kozima 1998, 2006, 2026a, 2026b].

The model contained an adjustable parameter n_n, assumed to be the density of the trapped neutrons. It is possible to compare the experimental and theoretical data in favorable cases when more than two observables are obtained in an experiment then the adjustable parameter n_n is determined by one of the observables and the value of n_n is used to calculate another observable theoretically. The theoretical value of the latter observable can be compared with the corresponding value of the observable determined by experiment to check the validity of the TNCF model.

4.1 Explanation of Experimental Results containing Nuclear Transmutation with Small Changes of Proton Numbers *Z*

In the early stages of the researches of CFP, there had been mainly observed excess energy generation accompanied with nuclear transmutations. The experimental data sets more than 50 had been analyzed by using the TNCF model and the result had been shown in Kozima's books published in 1998 and 2006 [Kozima 1998 (Figs. 11.2 and 11.3), 2006 (Tables 2.2 and 2.3)].

We have to notice the self-consistent, semi-quantitative explanation of the relation between the numbers N_a and N_b of observables a and b measured simultaneously. Using an adjustable parameter $n_{\rm n}$ in the TNCF model, the comparison of the ratio $N_a/N_b|_{th}$ determined by the model with the ratio $N_a/N_b|_{ex}$ determined by experiments gives conclusive evidence of the ability of the model. The agreement between two such observables as excess heat, tritium, helium 4 and neutron, presented in our book and papers (e.g., [Kozima 2016b, 2017]) clearly demonstrated the validity of the model.

4.2 Explanation of Experimental Results containing Nuclear Transmutation with Large Changes of Proton Number *Z*

Over time, experimental data on nuclear transmutation involving large changes in Z became available. The data with large changes of the proton number asked new development of the model to analyze the new data sets.

We extended the TNCF model to include the new demand of large changes of Z and the mass number A altogether. The idea is to consider the accumulation of the neutron Bloch waves at the boundary where they are reflected and superposed additively making the density of the trapped neutrons very large. Then we can assume high-density neutrons there as assumed in the simulation of the neutron star matter [Baym 1971, Negele 1973]. The neutron clusters ${}^{A}_{Z}\Delta$ composed of Z protons and $N = A - Z$ neutrons can be formed there. By doing so, we can gain more degrees of freedom regarding nuclear transmutation.

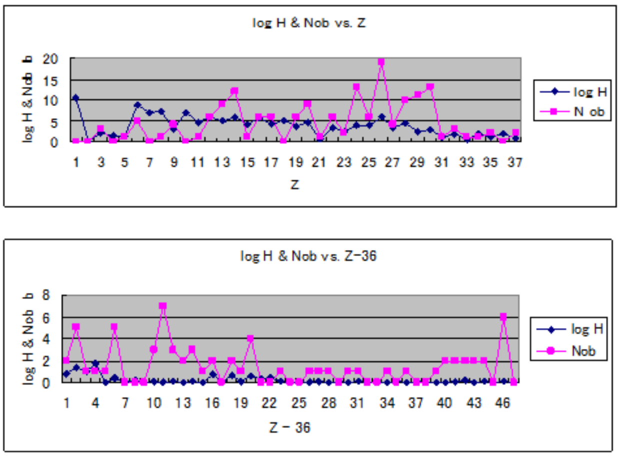

Fig. 3.1. Correspondence between the frequency $N_{\rm ob}$ observing elements in the CFP and the relative abundances $\log_{10}H$ of elements [Suess 1956] in the universe: (a) $Z = 3 - 38$ and (b) $Z = 39 - 83$ [Kozima 2006, 2012].

Fig. 3.1 shows a summary of experimental data on nuclear transmutation along with the relative abundances ($\log_{10}H$) of elements in the universe. Remarkable features seen in the figure is the peak at $Z = 26$ (Fe) and $Z = 82$ (Pb).

5. Conclusion

It goes without saying that science is an intellectual construct built on experimental evidence, but when we are in the midst of science, this fact is often forgotten and we tend to focus on other aspects of science, such as its applications and formal consistency.

Using the term "paradigm," which T. Kuhn used to describe the history of science, we could say that the root of this tendency is the tendency of scientists to rely too easily on paradigms prevailing at the time. However, as we have experienced in our research on CFP in these more than 35 years, this tendency is by no means admirable and should be avoided as much as possible.

With these questions in mind, I felt it was necessary to look back at the history of research to date and return to the essence of science to envision the future in order to understand the current state of CFP research.

The nuclear physics, one of the main branches of the solid state-nuclear physics, is a comparatively new science based in 1932 when the neutron was discovered and we know well its vivid development at hand. The brief history of the nuclear physics portrayed in this paper gave us the courage to take on the challenge of building a new science including the nuclear physics of the exotic nucleus.

The wide range and variety of experimental evidence obtained so far in the field of CFP teaches us the grandeur and difficulty of building the solid-state nuclear physics that is yet to be established.

However, considering the present state of the nuclear physics progressing on the experimental data scarcely obtaining with expensive and complicated apparatuses, we, scientists working in the field of the cold fusion phenomenon, are in a much more favorable position than nuclear physicists. Fortunately, we have found several laws, or regularities, in experimental data of physical observables [Kozima 2012] and also a model which can give qualitative explanations for them [Kozima 1998, 2006, 2013]. While we can't yet form a clear picture of what the final result will be, I'd say we've finally gotten a foothold.

References

[Alexandrov 1992] Yu. A. Alexandrov, *Fundamental Properties of the Neutron,* Clarendon Press, Oxford, 1992, ISBN 0-19-851735-1.

[Baym 1971] G. Baym, H.A. Bethe and C.J. Pethick, “Neutron Star Matter,” *Nuclear Physics*, **A175**, pp. 225 – 271 (1971).
[Casten 2000] R.F. Casten, *Nuclear Structure from a Simple Perspective,* 2nd Edition, Oxford University Press, 2000, ISBN 0-19-850724-0.
[Fleischmann 1989] M, Fleischmann, S. Pons and M. Hawkins, "Electrochemically induced Nuclear Fusion of Deuterium," *J. Electroanal. Chem*., **261**, 301 – 308 (1989), ISSN: 1572-6657.
[Jelley 1990] N.A. Jelley, *Fundamentals of Nuclear Physics,* Cambridge Univ. Press, Cambridge, 1990, ISBN 0-521-26994-6.
[Kozima 1998] H. Kozima, *Discovery of the Cold Fusion Phenomenon – Development of Solid State-Nuclear Physics and the Energy Crisis in the 21st Century –*, Ohtake Shuppan Inc., 1998, ISBN 4-87186-044-2. The “References” in this book is posted at the CFRL (Cold Fusion Research Laboratory) Website:
http://www.kozima-cfrl.com/Books/bookse/bookse.html
[Kozima 2006] H. Kozima, *The Science of the Cold Fusion Phenomenon*, *– In Search of the Physics and Chemistry behind Complex Experimental Data Sets –*, 1st Edition, Elsevier, Amsterdam, 2006, ISBN-13: 978-0-08045-110-7, ISBN-10: 0-080-45110-1.
[Kozima 2012] H. Kozima, “Three Laws in the Cold Fusion Phenomenon and Their Physical Meaning,” *Proc. JCF12* (Kobe, Japan, December 17 – 18, 2011), pp. 101 – 114 (2012), ISSN 2187-2260.
[Kozima 2013] H. Kozima, “Cold Fusion Phenomenon in Open, Nonequilibrium, Multi-component Systems – Self-organization of Optimum Structure,” *Proc. JCF13* 13-19, pp. 134 - 157 (2013), ISSN 2187-2260.
[Kozima 2016a] H. Kozima, “From the History of CF Research – A Review of the Typical Papers on the Cold Fusion Phenomenon –,” *Proc. JCF16,* **16-13,** pp. 116‐157 (2016), ISSN 2187-2260.
[Kozima 2016b] H. Kozima and K. Kaki, “The Cold Fusion Phenomenon and Neutrons in Solids,” *Proc. JCF16,* **16-14,** 158 – 198 (2016), ISSN 2187-2260.
[Kozima 2017] H. Kozima, T. Ohmori and M. Ohta, “Nuclear Transmutations in Critical and Supra-critical Electrolysis with Graphite, Pd, W, Re, Pt and Au Cathodes Analyzed by the TNCF Model,” *Proc. JCF17,* **17-12,** pp. 89‐147 (2017), ISSN 2187-2260.
[Kozima 2018] H. Kozima, “Nuclear Transmutations and Stabilization of Unstable Nuclei in the Cold Fusion Phenomenon,” *J. Condensed Matter Nucl. Sci.* **28**, 28 – 49 (2019), ISSN 2227-3123.
[Kozima 2019] H. Kozima, “On the 30th Anniversary of the Discovery of the Cold Fusion Phenomenon,” *Infinite Energy*, **145**･(May/June), pp. 28 – 34 (2019), ISSN 1081-6372.

[Kozima 2026a] H. Kozima, "In Search of Tritium – One of the Main Nuclear Products in the Cold Fusion Phenomenon in Solid State-Nuclear Physics –," *J. Cond. Matter Nucl. Science*, **41,** (2026), ISSN 2227-3123 (to be published).

[Kozima 2026b] H. Kozima, "The Cold Fusion Phenomenon in PdH_x and Detection of Tritium – A Historical Review of the Cold fusion Phenomenon (1) –," *Proc. JCF25,* pp. (2026), ISSN 2187-2260 (to be published).

[Molina 2021] I. Molina de la Pena, J. L. Calvo and R.F. Alvarez-Estrada, "Neutron waveguides: a proposal for slow neutrons confinement and applications in neutron optics," *Asian Journal of Physics*, 30, Nos 8 & 9, pp. 1289 – 1294 (2021), ISSN 0971-3093.

[Molina 2023] I. Molina de la Peña, "Neutron Optics: Characterization and Use of Neutron Waveguides," Ph.D. thesis, Universidad Complutense de Madrid (2023).

[Nakajima 1996] H. Nakajima, "*Robert Hooke: The Man Erased by Newton*," Asahi Shinbun Publishing Co., 1996, ISBN 4-02-259665-1 (in Japanese). The English citations of this book in this paper were made by H.K. with the assistance of *Google Translate*.

[Negele 1973] J.W. Negele and D. Vautherin, "Neutron Star Matter at Sub-nuclear Densities," *Nuclear Physics*, **A207**, pp. 298 - 320 (1973).

[Pavan 2025] M. Pavan, V. Raja and A.R. Barron, *Physical Methods in Chemistry and Nano Science* (Sec. 7.5), 2025, Rice University LibreTexts Project https://libretexts.org/

[Richtmyer 1976] F.K. Richtmyer, E.H. Kennard and J.N. Cooper, *Introduction to Modern Physics,* Sixth Edition (Revised), Tata McGraw-Hill Pub. Co. Ltd., New Delhi, 1976.

[Shull 1956] C.G. Shull and E.O. Wollan, "Applications of Neutron Diffraction to Solid State Problems," *Solid State Physics* Vol. **2**, Ed. Seitz and Turnbull, pp. 137 – 217, (1956), ISBN-10: 0126077029.

[Singh 2025] S. Singh, H. Bhatt, A. Gupta and M. Gupta, "Neutron standing wave at total reflection and neutron bandpass filter using periodic superlattices," *J. Appl. Phys*. **137**, 065301 (2025), ISSN 0021-8979.

[Steyerl 2020] A. Steyerl, *Ultracold Neutrons*, World Scientific Publishing Co., Singapore 2020, ISBN: 978-981-12-1270-3.

[Suess 1956] H.E. Suess and H.C. Urey, "Abundances of the Elements," *Rev. Mod. Phys*. **28**, pp. 53 – 74 (1956).

[Tervisidis 1990] F. Tervisidis, N. Tsagas, J.C. Bates, "Filling characteristics of a neutron bottle," *Physics Letters* A, Volume **148**, Issues 1–2, Pages 20-26 (1990), ISSN: 0375-9601.

A note without reviewing

The Existence of Long-Range Nuclear Forces

Kazuo Ooyama
Ooyama Power Inc., Tokyo, Japan
k2@ooyama-power.com

JCF25, March 2026

Abstract

Anomalously large neutron cross sections—both reaction and elastic scattering—that cannot be accounted for by conventional short-range nuclear forces based on Yukawa theory (effective range ∼2.5 fm) have long been observed. These anomalies have not been treated as unresolved problems: the large $1/v$ reaction cross sections were considered explainable through resonances, and the anomalously large elastic scattering cross section of ^{1}H relative to its nuclear size was considered explainable by scattering lengths. However, recent precise data from JENDL-5 (Japan Atomic Energy Agency) bring these explanations into contradiction. This paper first identifies these anomalously large cross sections as genuinely unresolved problems. We then postulate a long-range nuclear force that simultaneously accounts for both anomalies, and derive $V(r) = -N_A/r^4$ from the $1/v$ law using classical mechanics, determining N_A for each nuclide. Quantum mechanical simulation of ^{3}He using the two-dimensional Schrödinger equation (split-operator FFT method) at 250 eV, 1 keV, and 4 keV with the determined N_A reproduces both the $1/v$ law for absorption and the energy-independent behavior of elastic scattering, confirming the existence of this long-range nuclear force.

1 Introduction

In nuclear reaction cross-section measurements, E denotes the kinetic energy of the incident neutron and v its velocity. These are related by $E = \frac{1}{2}mv^2$, giving $v \propto \sqrt{E}$, or equivalently $\sqrt{E} \propto v$. Conventional nuclear physics recognizes short-range nuclear forces based on Yukawa theory [1], with an effective range of approximately 2.5 fm (1 fm $= 10^{-15}$ m).

The reaction cross sections of ^{3}He, ^{6}Li, ^{7}Be, and ^{10}B follow the $1/v$ law over 10^{-5}–10^4 eV, implying effective interaction radii far exceeding 2.5 fm. This contradiction has been ignored on the grounds that the Breit–Wigner formula [2] can explain the $1/v$ law through resonances. However, JENDL-5 [3] explicitly states that no resonance parameters exist for these nuclides. The $1/v$ law for these nuclides is therefore a genuinely unresolved problem that resonance theory cannot address.

Separately, the elastic scattering cross section of ^{1}H is 20.4 b over 10^{-5}–10^4 eV—more than 100 times the geometric cross section expected from the nuclear size. This has been explained using spin-dependent scattering lengths, but as discussed in Sec. 2.3, this explanation contains fundamental contradictions.

These two anomalies strongly suggest the existence of long-range nuclear forces distinct from the conventional short-range interaction.

2 Anomalous Neutron Cross Sections

2.1 $1/v$ reaction cross sections

Figure 1 shows the neutron cross sections of ^{3}He and ^{6}Li from JENDL-5. In both cases the reaction cross section (solid line) decreases in inverse proportion to $v \propto \sqrt{E}$—the $1/v$ law—over a wide energy range from 10^{-5} eV to 10^4 eV. The effective interaction radius, defined as $R_{\text{eff}} = \sqrt{\sigma_R/\pi}$, reaches 413 fm for ^{3}He and 173 fm for ^{6}Li at $E = 1$ eV. Since $\sigma_R \propto 1/\sqrt{E}$, the $1/v$ law gives $R_{\text{eff}} \propto E^{-1/4}$; at thermal energies ($E = 0.025$ eV), R_{eff} grows by a further factor of $(1/0.025)^{1/4} = 40^{1/4} \approx 2.5$, reaching approximately 1030 fm for ^{3}He and 430 fm for ^{6}Li—far exceeding the short-range nuclear force range of 2.5 fm.

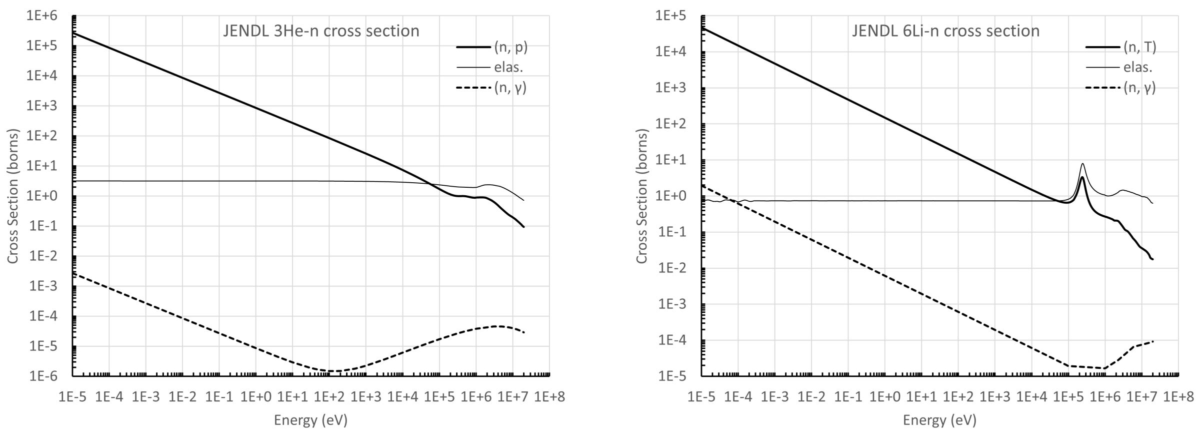

(a) ^{3}He (b) ^{6}Li

Figure 1: Neutron cross sections of (a) ^{3}He and (b) ^{6}Li from JENDL-5. Solid line: reaction cross section; thin line: elastic scattering; dashed line: radiative capture. Both reaction cross sections follow the $1/v$ law over 10^{-5}–10^4 eV.

The traditional explanation for the $1/v$ law is that slow neutrons spend more time near the nucleus and are therefore more likely to undergo nuclear reactions. Many researchers further assume that this behavior can be derived from the Breit–Wigner formula [2] through resonances. However, this qualitative "residence time" argument is not based on a derivation published in peer-reviewed literature, but is a common belief repeated in textbooks.

Furthermore, JENDL-5 explicitly states that no resonance parameters exist for ^{3}He, ^{6}Li, ^{7}Be, and ^{10}B; the $1/v$ law therefore remains a genuinely unresolved problem.

2.2 Correlation between reaction and elastic cross sections

Table 1 lists the reaction cross section σ_R and elastic scattering cross section σ_E at neutron energies near 1 eV for three nuclides that exhibit the $1/v$ law.

In conventional nuclear physics, the $1/v$ reaction cross section and the elastic scattering cross section are explained by independent mechanisms—the former through resonances or the residence time argument, the latter through spin-dependent scattering lengths.

Table 1: Reaction and elastic scattering cross sections from JENDL-5 near $E = 1$ eV.

Nuclide	E [eV]	σ_R [b]	σ_E [b]	σ_R/σ_E
^{3}He	1.000	846.4	3.135	270
^{6}Li	1.000	149.6	0.739	202
^{10}B	1.006	607.3	2.144	283

These two cross sections are therefore expected to be unrelated to each other. However, Table 1 shows a clear positive correlation: nuclides with a larger σ_R also have a larger σ_E, with the ratio σ_R/σ_E lying in the narrow range 200–283 for all three nuclides. This correlation strongly suggests that both cross sections share a common physical origin, and that a single long-range nuclear force can account for both simultaneously.

2.3 Energy-independent elastic scattering

Figure 2 shows the neutron cross sections of ^{1}H and ^{7}Be from JENDL-5. The elastic scattering cross section of ^{1}H is approximately 20.4 b and energy-independent over 10^{-5}–10^{4} eV. The proton charge radius is 0.84 fm; if the neutron has a comparable radius, the geometric cross section for a hard-sphere collision would be $\sigma_{\text{geo}} = \pi(0.84 + 0.84)^2 \approx 0.088$ b, roughly 230 times smaller than the observed value. As shown in Fig. 2(b), ^{7}Be exhibits an anomalously large elastic scattering cross section of 384.4 b at 0.025 eV, which likewise cannot be explained by short-range nuclear forces alone.

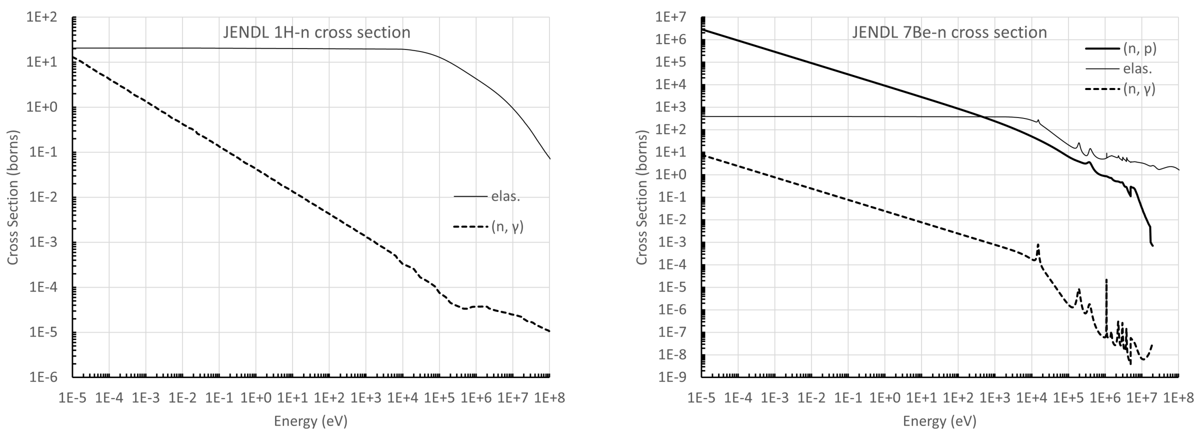

(a) ^{1}H (b) ^{7}Be

Figure 2: Neutron cross sections of (a) ^{1}H and (b) ^{7}Be from JENDL-5. (a) The elastic scattering cross section of ^{1}H is constant at 20.4 b over 10^{-5}–10^{4} eV; no reaction cross section exists for this nuclide. (b) ^{7}Be shows a reaction cross section of 56,777 b and an elastic scattering cross section of 384.4 b at 0.025 eV.

The standard explanation for the ^{1}H elastic scattering cross section invokes spin-dependent scattering lengths. The neutron and proton each carry spin 1/2, giving a triplet state (total spin 1, statistical weight 3) and a singlet state (total spin 0, statistical weight 1). Using the triplet scattering length $a_t \approx 2.82$–5.42 fm and the singlet scattering length $a_s \approx \pm 23$–23.7 fm, the cross section is written as

$$\sigma = 3\pi a_t^2 + \pi a_s^2. \tag{1}$$

The singlet scattering length a_s is back-calculated from the experimental value of 20.4 b itself, so agreement with experiment is guaranteed by construction rather than by independent prediction.

This explanation contains fundamental contradictions. First, it does not explain why a_s far exceeds the 2.5 fm effective range of the short-range nuclear force. Second, thermal neutrons have a de Broglie wavelength of $\sim 1.81 \times 10^6$ fm; the transverse extent of such a wave far exceeds the ~2.5 fm range of the short-range nuclear force, so the vast majority of the wavefront passes the nucleus without entering the region where the short-range force acts. A short-range force alone should therefore produce a *smaller* cross section at longer wavelengths, contrary to observation. Third, the same framework cannot explain the 384.4 b elastic scattering cross section of ^{7}Be. These contradictions confirm that the energy-independent elastic scattering cross section is also a genuinely unresolved problem.

3 Derivation of the $-N_A/r^4$ Potential

3.1 Classical derivation from the $1/v$ law

We seek a power-law central potential $V(r) = -N_A/r^n$ such that the resulting reaction cross section reproduces the $1/v$ law. Using classical orbital mechanics—the same approach as deriving the Bohr radius—the critical orbit condition gives a reaction cross section of the form

$$\sigma_R \propto \left(\frac{N_A}{E_0}\right)^{2/(n+1)}, \tag{2}$$

where E_0 is the neutron kinetic energy in the laboratory frame. Demanding $\sigma_R \propto E_0^{-1/2}$ uniquely fixes $n = 4$, giving $V(r) = -N_A/r^4$. The reaction cross section is then

$$\sigma_R = \pi\sqrt{\frac{4M}{M-m} \cdot \frac{N_A}{E_0}}, \tag{3}$$

where M is the target nucleus mass and m the neutron mass.

3.2 Determination of N_A

Applying Eq. (3) to JENDL-5 cross-section data, the coefficient N_A is determined for each nuclide with no free parameters (Table 2). Center-of-mass kinematics are used throughout.

Table 2: Long-range nuclear force coefficient N_A determined from JENDL-5 data for each nuclide.

Nuclide	E [eV]	σ_R [b]	M [u]	m [u]	N_A [J m^4]
^{3}He	1.000	846.43	3.016029	1.008665	1.935×10^{-71}
^{6}Li	1.000	149.55	6.015122	1.008665	7.555×10^{-73}
^{7}Be	1.062	8722.8	7.016929	1.008665	2.808×10^{-69}
^{10}B	1.006	607.32	10.012937	1.008665	1.354×10^{-71}

The values of N_A span three orders of magnitude, consistent with a species-dependent force strength expected for a nuclear rather than electromagnetic interaction. For comparison, the electric polarizability of the neutron yields $C_{\rm EM} \sim 5 \times 10^{-76}$ J m^4 for ^{3}He, five orders of magnitude smaller than N_A, ruling out an electromagnetic origin.

4 Quantum Mechanical Verification

4.1 Simulation setup

To verify Eq. (3), we solved the two-dimensional time-dependent Schrödinger equation numerically for a neutron wave packet incident on a stationary ^{3}He nucleus. The total potential is complex,

$$V(r) = V_{\mathrm{real}}(r) + iV_{\mathrm{imag}}(r), \tag{4}$$

where the real part drives elastic scattering and the imaginary part drives absorption. For ^{3}He, where the reaction cross section greatly exceeds the elastic scattering cross section ($\sigma_R/\sigma_E \approx 270$), absorption dominates. We therefore set

$$V_{\mathrm{real}}(r) = 0, \quad V_{\mathrm{imag}}(r) = -\frac{N_A}{r^4}, \tag{5}$$

with $N_A = 1.935 \times 10^{-71}$ J m^4. The $-N_A/r^4$ singularity at $r = 0$ is avoided in practice because the nearest grid point to the nucleus is determined by the grid spacing, which is much larger than the nuclear radius at all three energies. In this model, the imaginary potential drives absorption and simultaneously deflects the passing neutron wave, giving rise to elastic scattering as well, so both cross sections are obtained from a single calculation. For purely elastic nuclides such as ^{1}H, $V_{\mathrm{imag}} = 0$ and $V_{\mathrm{real}} \neq 0$.

The split-operator FFT method was used on a uniform Cartesian (x, z) grid executed on Google Colaboratory. Absorbing boundary layers at all grid edges suppressed spurious reflections. The computational domain and time step were scaled with the de Broglie wavelength at each energy so that each calculation samples the same physical geometry relative to the neutron wavelength. Table 3 lists the computational parameters for each energy.

Table 3: Computational parameters for the n–^{3}He simulation at three energies. λ: de Broglie wavelength; σ_0: initial wave-packet width; z_0: initial packet center; dt: time step.

Parameter	250 eV	1 keV	4 keV
N_A [J m^4]		1.935×10^{-71}	
λ [fm]	1810	905	452.5
σ_0 [fm]	2000	1000	500
Domain [nm]	40×20	20×10	10×5
Grid $N_x \times N_z$	2293×1380	1621×976	1147×690
z_0 [nm]	-5	-2.5	-1.25
$t_{\max}$ [zs]	48000	12000	3000
dt [zs]	2	0.5	0.125

4.2 Results

Figure 3 shows the total probability density $|\psi|^2$ and the scattered wave $|\psi_{\mathrm{sc}}|^2$ at 1 keV at the final time $t_{\max} = 12000$ zs (1 zs = 10^{-21} s). The 250 eV and 4 keV patterns are geometrically similar and are omitted.

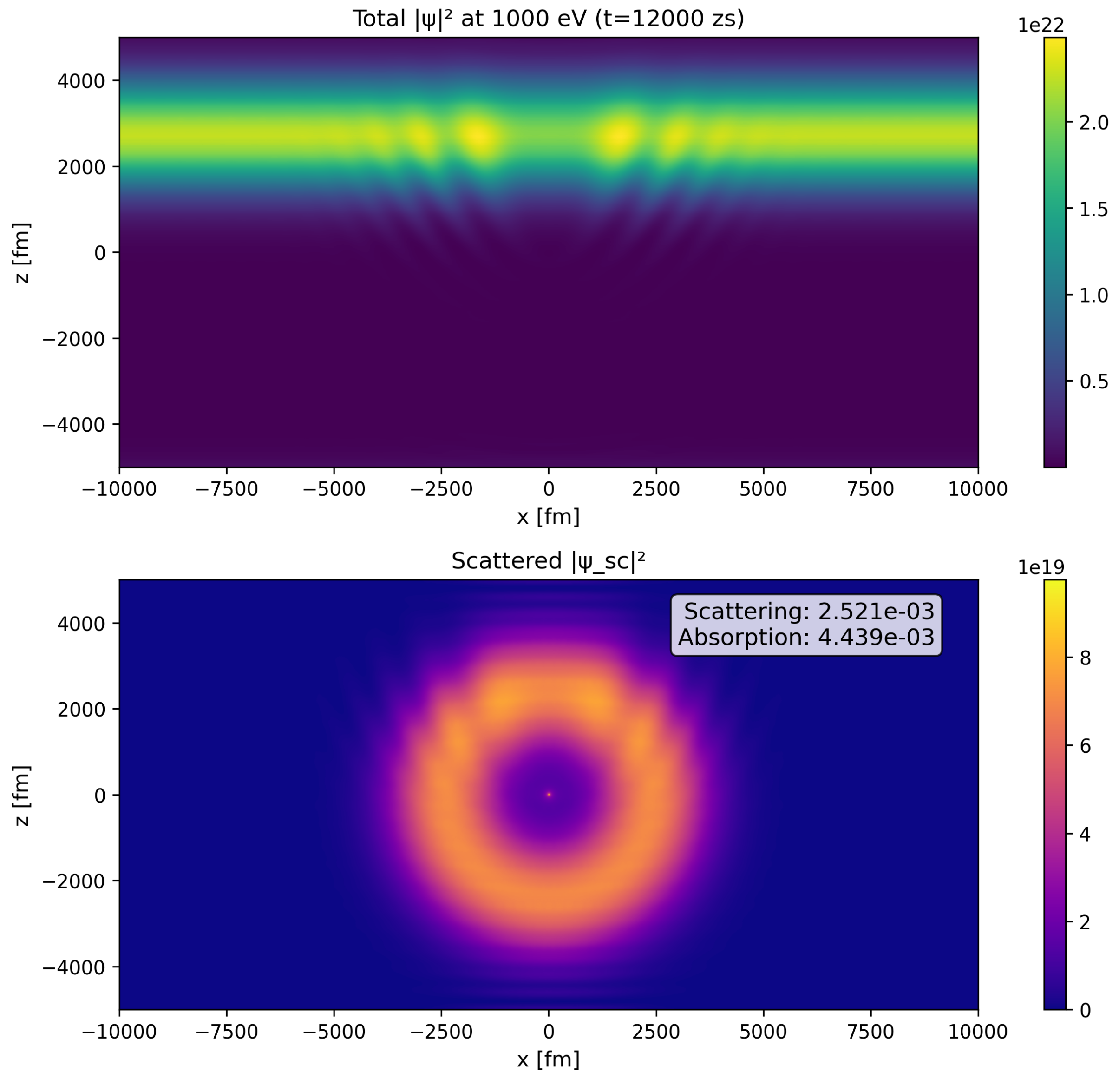

Figure 3: Simulated neutron probability density $|\psi|^2$ (upper) and scattered wave $|\psi_{\rm sc}|^2$ (lower) for n–^{3}He at 1 keV ($N_A = 1.935 \times 10^{-71}$ J m^4). The ^{3}He nucleus is at the center; the neutron wave propagates in the $+z$ direction. The shadow downstream of the nucleus reflects absorption.

Table 4 compares the simulation results with JENDL-5 values. The simulation cross-section lengths [fm] are the two-dimensional analogs of cross sections; direct comparison with JENDL-5 values in barns requires a three-dimensional calculation.

Table 4: Simulation results for n–^{3}He compared with JENDL-5. Simulation values are two-dimensional cross-section lengths [fm]; JENDL-5 values are three-dimensional cross sections [b]. The rightmost columns give the ratio of each quantity to its value at 4 keV, confirming $1/v$ scaling of absorption and energy-independence of elastic scattering.

	Simulation [fm]		JENDL-5 [b]		Ratio to 4 keV	
Energy	Scatter.	Absorp.	σ_E	σ_R	Scatter.	Absorp.
250 eV	46.84	162.96	3.10	52.00	1.092	4.069
1 keV	50.42	88.78	3.04	25.57	1.175	2.217
4 keV	42.91	40.05	2.95	12.18	1.000	1.000

Three conclusions follow from Table 4. First, the absorption cross-section length decreases approximately as $1/\sqrt{E}$ (162.96, 88.78, 40.05 fm at 250 eV, 1 keV, 4 keV), reproducing the $1/v$ law consistent with the JENDL-5 σ_R values. Second, the scattering cross-section length is nearly constant (46.84, 50.42, 42.91 fm), reproducing the energy-independent elastic scattering consistent with the JENDL-5 $\sigma_E \approx 3.0$ b. Third, the $-N_A/r^4$ potential derived by classical mechanics is thus confirmed quantum mechanically.

Because the calculation is two-dimensional, direct quantitative comparison with JENDL-5 values in barns is not possible at this stage. Collaboration using high-performance computing for full three-dimensional calculations, including lower neutron energies, is sought.

5 Discussion and Conclusion

Detailed neutron cross-section data from JENDL-5 reveal two anomalies that conventional nuclear physics has left unresolved. The $1/v$ reaction cross sections of ^{3}He, ^{6}Li, ^{7}Be, and ^{10}B cannot be explained by resonance theory because JENDL-5 lists no resonance parameters for these nuclides. The energy-independent elastic scattering cross section of ^{1}H cannot be explained by spin-dependent scattering lengths without introducing a singlet scattering length that far exceeds the effective range of the short-range nuclear force, and without addressing the fact that the de Broglie wavelength of thermal neutrons vastly exceeds the nuclear radius.

We have shown that a long-range nuclear force $V(r) = -N_A/r^4$, derived from the $1/v$ law by classical mechanics, provides a common microscopic origin for both anomalies. The coefficient N_A is determined from JENDL-5 data with no free parameters for each nuclide. Quantum mechanical simulation for ^{3}He at 250 eV, 1 keV, and 4 keV confirms that this potential reproduces both the $1/v$ scaling of the absorption cross section and the energy-independent behavior of the elastic scattering cross section.

The existence of a long-range nuclear force has direct implications for condensed-matter nuclear science. The $-N_A/r^4$ interaction modifies the effective potential between deuterons in metal lattices, providing a theoretical foundation for DD binary nuclei and DDD triple-nucleus states discussed in a companion paper [4]. A full theoretical derivation and extended three-dimensional numerical analysis has been deposited as a preprint [5] and will be submitted to *Physical Review C*.

References

[1] H. Yukawa, Proc. Phys. Math. Soc. Jpn. **17**, 48 (1935).

[2] G. Breit and E. P. Wigner, Phys. Rev. **49**, 519 (1936).

[3] O. Iwamoto, N. Iwamoto, S. Kunieda, F. Minato, S. Nakayama, Y. Abe, et al., J. Nucl. Sci. Technol. **60**, 1 (2023).

[4] K. Ooyama, "Nuclear physics of metal lattice fusion reactors," JCF25, 2026 (companion paper).

[5] K. Ooyama, "Long-range nuclear force of $-N_A/r^4$ form," Research Square preprint, `https://doi.org/10.21203/rs.3.rs-9458930/v1` (2026).

A note without reviewing

Nuclear Physics of Metal Lattice Fusion Reactors:

金属格子型核融合炉の核物理

(Experimental Evidence and a Proposed DD-Binary/DDD-Trimer Reaction Model)

（実験的証拠および提案される DD 連星核／DDD3 連星核反応モデル）

Kazuo Ooyama

Ooyama Power Inc., Tokyo, Japan k2@ooyama-power.com

JCF25, March 2026

Abstract

We report experimental startup of light-hydrogen and deuterium metal lattice fusion reactors using a Pd sample doped with ^{6}Li ions at 75° C. In the light-hydrogen experiment, continuous γ-ray emission (>0.1 μSv/h) lasting 1.5 h was confirmed via a nuclear chain reaction. In the deuterium experiment, neutron bursts reaching 52.4 μSv/h (5-min integrated) were observed. We argue that conventional DD fusion reactions alone cannot account for ^{6}Li regeneration (Okamoto et al.) nor for high-energy protons and α particles in TiDx experiments (Kasagi et al.). We propose DD binary nuclei and DDD trimer nuclei form in metal lattices via a long-range r^{-4} nuclear force. Accumulation of DDD trimers followed by d-ion impact explains periodic neutron bursts and ^{6}Li regeneration through high-energy (>20 MeV) secondary products.

本稿では、75℃で ^{6}Li イオンをドープした Pd 試料を用いた軽水素および重水素金属格子核融合炉の実験的起動について報告する。軽水素実験では、核反応の連鎖反応を介して、1.5 時間にわたる連続 γ 線放出（>0.1 μSv/h）が確認された。重水素実験では、5 分間積算で 52.4 μSv/h に達する中性子バーストが観測された。従来の DD 核融合反応だけでは、^{6}Li の再生（岡本ら）や TiDx 実験における高エネルギー陽子および α 粒子（笠木ら）を説明できないと考える。我々は、長距離 r^{-4} 核力によって金属格子中に DD 連星核および DDD3 連星核が形成されると提唱する。 DDD3 連星核の蓄積とその後の d イオン衝突により、周期的な中性子バーストと高エネルギー（>20 MeV）二次生成物による ^{6}Li の再生成が説明される。

1. 序論：「死後の熱」と金属格子型核融合の原理

Fleischmann と Pons（1993）は、Pd 電極を用いた重水電解実験においての電解セル(JCF24 の proceedings で引用した p76 の Fig. 3[7])の 4 台のうち 1 台が、電解液がなくなり電解電流が流れなくなってから 3 時間 100℃の温度が維持され発熱が継続したことを

「死後の熱（heat after death)」のタイトルの論文で報告している［1]。この時の 16.6×10^6 秒 ＝192 日の電解（この間の電流量と温度の変化の様子を示す図[8]は同 p75 の Fig. 2[7]に引用した。）の最後の 60000 秒の温度変化の図［1] (同 p74 の Fig. 1[7]で引用している。）のセルがドライになった後の最後の 3 時間がこの「死後の熱」を表している。

温度が 100℃になって電解液を消失してから、この「死後の熱」が発生しているが、この電解セルは大気開放と書かれている[8]。我々は水素圧力が 0.02bar の時の Pd-H 状態図（JCF24 の proceedings の p78 の Fig.5[7]）を作成したが、40℃以上では高 D 濃度の α’相はできない。つまり「死後の熱」は Pd の D 濃度の低い α 相で起きており、発熱には高 D 濃度が有利とする Pons らの推定はミスリードであった。

我々は「死後の熱」の発熱の原理を次のように推定した。起点は、熱中性子（0.025 eV）と ^{6}Li 核との反応である。^{6}Li は ^{235}U の 1.4 倍（940b）の熱中性子反応断面積を持ち、常温での核反応が可能である[2]。^{6}Li(n, t）α反応で生成されたイオンが結晶格子のチャネルに拘束され、格子間に固溶した水素（重水素）核に弾性散乱で d イオンを生成し、その d イオンが核融合連鎖反応を引き起こす（JCF23proceedings の p43 の Fig.4[6]参照)。発生したイオンの運動エネルギーが金属の阻止能（stopping power）を介して熱に変換される。実験炉では熱中性子の偶発的な反応に依存できないため、α線源を用いた。

2. 実験

2.1 使用サンプルと実験系

99.95%純 Pd サンプルを、2% H_2 を含む Ar ガス中で 1300° C・1 時間焼鈍し、結晶を粗大化した。次に 180keV の ^{6}Li イオンを 5.1×10^{15} 個/cm2 ドープした（深さ約 0.5 μm、最大 0.177 mol%)。サンプルを熱伝達離壁を介して密閉容器内に設置し、着火用α線源を配置した。(概略図は JCF23 の proceedings で引用した p57 の Fig. 19[6], 炉の写真は JCF24 の proceedings p81 Fig. 7, p82 Fig. 8[7］参照）

ガンマ線線量率は、ガンマ線サーベイメーター（テクノ AP 株式会社製、TC100S；検出範囲：100 keV～1.5 MeV、線量率範囲：0.001～50 μSv/h、感度：2,500 cpm/μSv/h）を用いて測定した。この装置にはデータロギング機能がないため、測定値は観測時にオペレーターが手動で記録した。中性子線量率は、中性子サーベイメーター（富士電機株式会社製、NSN31045-111YY-S；エネルギー範囲：0.025 eV～15 MeV、検出器：有機混合ガス比例計数管、減速材：ポリエチレン、線量率範囲：1 μSv/h～99.99 mSv/h）を用いて測定した。中性子サーベイメーターは 5 分間隔でデータを記録した。バックグラウンドは 0.020～0.050 μSv/h であったが、これは本機器の有効測定範囲（下限 1 μSv/h）を下回っており、実質的にバックグラウンドは検出限界以下であったことを示す。

2.2 実験①：軽水素金属格子型核融合炉の起動

ロータリーポンプにより H2 ガス雰囲気でベーキング中 2019 年 1 月 23 日 8 時に 75° C

に設定温度を上げて、翌 24 日 10 時 31 分に γ 線が 0.400 μSv/h 以上に達した。その後約 1.5 時間にわたって 0.100μSv/h 以上の連続した γ 線放出が確認された。このとき真空圧は 0.1〜0.2Pa で変動していた（ベーキング中であり平衡水素圧とは言えない。)。推定される連鎖反応は以下の通りである：

X + 1H → X + p （弾性散乱） (a)

p + ^{6}Li → ^{3}He (2.3 MeV) + α (1.7 MeV) （99.9968%） (b)

p + ^{6}Li → ^{7}Be + γ (5.6 MeV) （〜0.0032%） (c)

α線源からのαイオン X が格子チャネル内の ^{1}H 核に衝突して p イオンを生成し（式 a)、その p が ^{6}Li 核に衝突し、α イオンと ^{3}He イオンを生成し（式 b)、生成したイオンが次の X となり連鎖反応を継続させる。式 b の核反応に伴い一定の割合で式 c の核融合反応が起き、この γ 線が検出されたものと思われる。

^{6}Li(p,γ)^{7}Be チャネルの^{6}Li(p,^{3}He)^{4}He に対する分岐比は Ep ≈ 400 keV で 3.2×10^{-5} である（EXFOR データ：Kwon ら[10]および Bashkin ら[11])。連鎖増幅なしで推定した γ 線発生率は約 3×10^{-18} s^{-1}であるのに対し、TC100S（感度 2,500 cpm/μSv/h、検出器立体角比 4×10^{-4}、炉体とヒーターを含めて約 1 cm 厚の SUS316 としたときの壁透過率 50%、CsI(Tl)検出効率 26%）で観測された 0.400 μSv/h から逆算したγ線発生率は約 3×10^5 s^{-1}であり、両者の差は 22 桁に達する。これは連鎖反応なしには観測結果を説明できないことを示す。つまり 1.5 時間の連続 γ 線放出が確認できたことは、軽水素炉でも核融合連鎖反応が成立することを示唆している。

上記連鎖反応を仮定した場合、(c)式で 3×10^5 s^{-1}の γ 線が発生しているとしたときの (b)式の反応数はその 99.9968/0.0032 倍になり、その推定発熱量は約 0.001 W になる。現在の検出限界以下であることは観察結果と一致する。(軽水素実験における分岐比の導出、立体角・検出効率を含む定量的なγ線発生率の推定、および推定発熱量計算の詳細については文献[12]Sec. 4. 1 を参照願いたい。)

2.3 実験②：重水素金属格子型核融合炉の起動

同日、軽水素による起動が成功した後、同サンプルに対して 75° C のベーキング完了後、14 時 58 分からマスフローメーターで重水素ガスを供給しはじめ、断続的に 5 回の重水素ガスを供給し総供給量 0.258cc に達し、サンプルに固溶するのを待っているときγ線放出が先行し中性子爆発が発生した。全量が Pd に固溶したとすると D/Pd 原子比 0.0046mol%相当である（実際には表面付近の濃度がより高いと思われる。)。

成果：重水素金属格子型核融合炉の起動（中性子爆発の発生）を確認した(中性子発生の証拠としての記録データは JCF24 の proceedings の p84 の Fig.9[7]参照)。発熱は確認できなかった。既知の DD 核融合反応のみではこの中性子の爆発的発生が説明できない（後述)。

表 1 重水素炉起動時の中性子線量計測記録（2019 年 1 月）

日時	種別	5 分当たりの計測値
1 月 24 日 19:38	最大中性子爆発	52.4 μSv/h（補正カウント 3513.5/5 分）
1 月 26 日 09:03	中性子バースト	16 μSv/h（補正カウント 100.5/5 分）
1 月 27 日 17:35	中性子バースト	3.02 μSv/h（補正カウント 37.5/5 分）

3.既知の反応式では説明できない現象

3.1 既知の DD 核融合反応

通常の DD 核融合の主反応と二次反応を以下に示す。

$d + {}^{2}H \rightarrow {}^{3}H$ (1.0 MeV) + p (3.0 MeV) （50%） (d)

$d + {}^{2}H \rightarrow {}^{3}He$ (0.8 MeV) + n (2.5 MeV) （50%） (e)

$d + {}^{2}H \rightarrow {}^{4}He + \gamma$ (23.8 MeV) （0.001%） (f)

${}^{3}H + {}^{2}H \rightarrow \alpha$ (3.5 MeV) + n (14.0 MeV) (g)

${}^{3}He + {}^{2}H \rightarrow \alpha$ (3.7 MeV) + p (14.7 MeV) (h)

これらの反応だけであれば安定した反応が継続し、中性子も安定して発生するはずである。ところが、実験②では中性子が爆発的に発生する現象が起きている。

3.2 TiDx への D イオン照射実験における異常粒子の観測

Uneme et al.（JCF2-20）による TiDx(重水素を固溶させたチタン金属）への低エネルギー重陽子線照射実験［3］と、Kasagi et al.（1995）による 150keV 重陽子線照射実験［4］において、通常の DD 核融合では生成されないエネルギーを持つ粒子が確認されている：（1）17.2MeV 以下の陽子線、（2）6.7 MeV 以下の α 線（JCF23 の proceedings で引用した p52 の Fig.13[6］参照）、（3）4.75 MeV の ${}^{3}H$ および ${}^{3}He$。これらは 1 次・2 次 DD 反応では説明できない（JCF23 の proceedings で引用した p51 の Fig. 12[6］参照）。

3.3 Pd 陰極における ${}^{6}Li$ 生成の証拠

中田ら（1992）による SIMS データ［5］(JCF24 の proceedings で引用した p79 の Fig.6[7]参照)は、電解中に発熱も中性子も検出されなかった Pd-5 サンプルにおいて、${}^{6}Li/{}^{7}Li$ 比が自然存在比（7.5: 92.5）から表面から 5 μm 付近で 1 ：1 に変化していることを示した。電解中に何も起きなかったことから、${}^{6}Li$ が生成されたのは電解終了後の「死後の熱」反応によるものと判断できる。ところが通常の核反応では ${}^{6}Li$ は生成されないのである。

本章で列挙したこれら既知の反応式では説明できない 3 つの現象は、恐らく個別の現象ではなく、共通した現象による結果として生じるものと考える。

4. 3 体核融合と連星核形成理論

4.1 3 体核融合反応

§3.2 で示した異常粒子（17.2 MeV 以下の p、6.7 MeV 以下の α、4.75 MeV の ^{3}H および ^{3}He）の起源を検討する。§3.1 で示した通常の DD 核融合の 1 次反応（式 d,e,f）および 2 次反応（式 g,h）では、生成粒子のエネルギーはそれぞれ p: 3.0 MeV、n: 2.5 MeV、α: 3.5〜3.7 MeV、p: 14.7 MeV が上限であり、17.2 MeV 以下の陽子や 6.7 MeV 以下の α を説明することはできない。したがって、これらの異常粒子は 3 個以上の D 核が関与する多体核反応の産物と考えられる。DD 核反応は一瞬で終わるので、同時に 3 つの D 核が 1 点に集合して 3 体核融合が起きる可能性はないと言える。金属内では、D 核に d イオンが衝突する際、強い相互作用による核融合に至らない弾性衝突において、長距離核力（文献[9]）が 2 つの D 核を互いに拘束し、DD 連星核（DD binary）を形成すると考えられる。この束縛状態の物理的根拠については 4.2 節で論じる。この DD binary は、安定状態で格子間原子として外乱が働かないため、3 つ目の D 核と反応するまで状態を保持できると考えられる。この DD binary に 3 つ目の d イオンが入ることで下記の DDD3 体核反応を起こすと考えることで、上述の異常粒子を説明することができる：

d + DD binary → ^{5}He (3.45 MeV) + p (17.2 MeV) (i)

→ ^{3}H (4.7 MeV) + ^{3}He (4.7 MeV) (j)

→ α (7.9 MeV) + D (15.8 MeV) (k)

式 i〜k は Uneme らや Kasagi らが観測した粒子エネルギー（17.2 MeV 以下の p、6.7 MeV 以下の α、4.75MeV の T と ^{3}He）と一致する。

4.2 DD 連星核（二核子束縛状態）の形成

原子を構成する電子は、光子放出という唯一の脱励起チャンネルを介して、原子核に対して安定準位に落ち着くことができる。γ 線は光子の一種であり、光子は質量を持たないが運動量 p=E/c を持つため、エネルギーと運動量の保存則を満たしながら束縛状態へ遷移すること自体は可能である。(f)式（d + 2H → 4He + γ, 23.8 MeV, 0.001%）で実証されているように、放射捕獲自体は核子系でも起こり得る。しかし電子の場合と異なり、核子系では強い相互作用に基づく粒子放出チャンネルが競合できる場合、電磁多重極遷移はそれらに比べて一般に確率が低い。通常の真空中では D と D の間に量子化条件を満たす DD 連星核（DD binary）のような束縛状態が存在するとしても、放射捕獲のみに依存した DD binary 形成は確率的に極めて起こりにくい。一方、金属内では阻止能とフォノンを介した運動量・エネルギー移行という、より高速かつ高確率な経路が追加されるため、DD binary への遷移が現実的な速度で進行すると考えられる。

この DD binary は、安定状態で格子間原子として収まり、外乱が働かないため 3 つ目の D 核と反応するまで状態を保持できると考えられる。

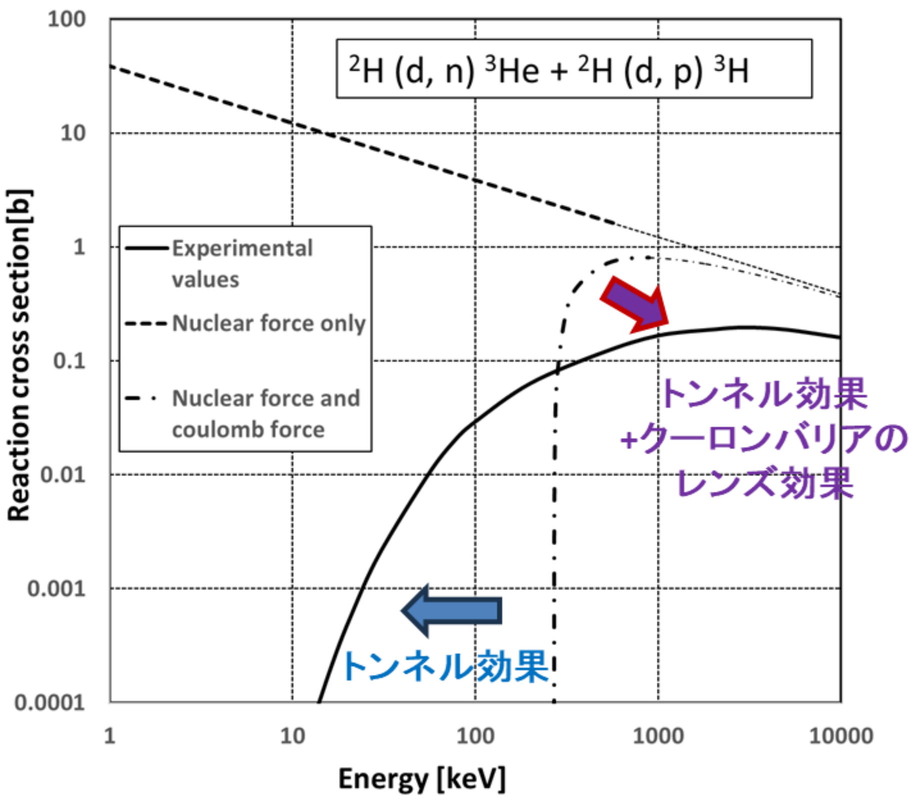

図 1 DD 核融合反応断面積の比較。実線：実験値。点線：長距離核力ポテンシャル En = −NA/r^4（NA = 187.3 MeV·fm^4）のみを考慮した場合の断面積（文献[9]のポテンシャルに基づく定性的推定）。一点鎖線：長距離核力ポテンシャルにクーロンポテンシャルを加えた場合の断面積。クーロン障壁のピークは L = 8 fm で約 67 keV（重心系 269 keV 相当）。

通常の Yukawa 型短距離核力ポテンシャルでは、DD 系の量子化条件を満たす束縛状態は形成されない（クーロン障壁内側での引力が不十分なため）。一方、我々は JENDL-5 の中性子断面積データにおける未解決の異常——反応断面積の 1/v 則と弾性散乱断面積のエネルギー非依存性——から長距離核力ポテンシャル En = −NA/r^4（NA = 187.3 MeV·fm^4）を導出している（詳細は文献[9]参照）。

図 1 は、このポテンシャルを用いて DD 核反応断面積を定性的に推定した結果と実験値の比較である。点線：長距離核力ポテンシャルのみの場合、一点鎖線：クーロンポテンシャルを加えた場合、実線：実験値。長距離核力とクーロン力の合成ポテンシャルにおけるクーロン障壁のピークは L = 8 fm で高さ約 67 keV（重心系で 269 keV 相当）であり、この障壁の内側に量子化条件を満たす準安定な束縛状態が存在し得る。

数値 Schrödinger 方程式による探索（進行中）では、l = 0（S 状態）の n = 1 において R = 2.105 fm に束縛状態の候補が見出されたが、ポテンシャルエネルギー −4.43 MeV に対

して運動エネルギーが 18.73 MeV と大きく、存在時間が短いと考えられる。より安定な候補として l = 1（P 状態)、S = 1、n = 1 の状態が挙げられる。ボゾン（D 核はスピン 1）の対称性条件(−1)^l × (−1)^S = +1 を満たすとともに、通常の電子軌道とは異なり、引力が距離とともに急激に減少する r^{-4}型ポテンシャルでは低量子数ほど安定軌道が障壁に近づく（外側になる）ため、n=1 が最も安定な候補となる。

波動関数の詳細な検討は今後の課題である。

4.3 DDD3 連星核の形成と^{6}Li 再生成

D 核（重陽子）はスピン 1 のボゾンであり、パウリ排他原理の制約を受けないため、複数の D 核が同一の量子状態を占有することが原理的に許容される。このため、DD 連星核にさらに d イオンが入射した場合、3 体のボゾン系として DDD3 連星核（DDD trimer）が形成される可能性がある。この DDD3 連星核にさらに d イオンが入射した場合の反応式を以下に列挙する。これらはいずれも 4D の静止質量（8.05640 u）と生成核の質量との差から計算される Q 値と各粒子のエネルギーの合計が一致しており、エネルギー保存則を満たしている：

d + DDD trimer → ^{6}Li (6.3 MeV) + D (19.0 MeV)　　(l)

d + DDD trimer → 2α（23.8 MeV × 2）　　(m)

d + DDD trimer → ^{7}Li (3.8 MeV) + p (26.5 MeV)　　(n)

d + DDD trimer → ^{7}Be (3.6 MeV) + n (25.1 MeV)　　(o)

§3.3 の中田らの^{6}Li/^{7}Li 比変化（自然存在比 7.5:92.5 から約 1:1 への変化）と整合する^{6}Li 生成の経路として、式(l)が存在する。通常の DD 核融合反応（式 d〜h）では^{6}Li は生成されないことから、式(l)は中田らの SIMS データの唯一の説明となる。式 n, o で生成する ^{7}Li・^{7}Be はさらに以下の二次反応を起こし得る：

^{7}Be → ^{7}Li + ν_e （電子捕獲，半減期 53.2 日）

d + ^{7}Li → ^{5}He (6.36 MeV) + α (7.96 MeV)

^{5}He → α（0.18 MeV) + n (0.73 MeV) （極めて短時間で崩壊）(p)

5. 中性子爆発のメカニズム

中性子バーストの周期的発生は以下の 3 段階モデルで説明できる。

【蓄積期】

格子チャネルを通過する α 線源（8,000 Bq、毎秒約 8,000 個の α 粒子）からの α イオンが、格子間に拡散した D 核と衝突して安定的に d イオンを生成すると、以下の 2 段階反応が進行する。

d + ^{2}H → DD binary (長距離核力[9]による n=1（P 状態)、S=1 の束縛状態)

d + DD binary → DDD trimer （D 核はスピン 1 のボゾンでありパウリ排他原理の制約

を受けないため、3 体ボゾン束縛状態が原理的に許容される）

この期間は DDD3 連星核が格子間に蓄積されていく。DDD3 連星核に d イオンが衝突するまでは式(l)〜(o)の反応が起きないため、反応は穏やかで中性子発生は少ない。

【爆発期】

DDD3 連星核密度が閾値に達すると、式 l〜o により 20 MeV クラスの高エネルギーイオンが多数生成される。高エネルギーイオンは 1 つで多くの D 核に衝突してさらに多くの高エネルギーd イオンを生成し、連鎖反応が急速に活発化する。この過程で中性子は主に以下の反応から放出される：

（1）式(e)　$d + {}^{2}H \rightarrow {}^{3}He + n$ (2.5 MeV)

（2）式(i)で生成した ^{5}He の式(p)による崩壊：n (0.73 MeV)

（3）式(o)　$d + DDD \rightarrow {}^{7}Be + n$ (25.1 MeV)

（4）式(o)で生成した ^{7}Be が式(p)の二次反応を経て放出：n (0.73 MeV)

特に式(o)による 25.1 MeV 中性子は通常の DD 核融合反応では生成されないエネルギーであり、このピークの検出が本モデルの実験的検証に有効である。

【回復期】

DDD3 連星核の数が減少すると連鎖反応が穏やかになり、再び蓄積期に戻る。このモデルは観測された「複数回の中性子バースト（表 1)」と「バースト間の静穏期」を一つの機構で説明する。また、^{6}Li が式(l)によって再生成されるため、重水素炉では D_2ガス供給のみで長期連続運転が原理的に可能と予測される。

6. 今後の課題と展望

（1）波動関数による連星核確認：数値 Schrödinger 方程式（Numerov 法・行列固有値法）による長距離核力ポテンシャル下での DD 連星核の束縛状態探索（進行中)。

（2）中性子エネルギースペクトル計測：式 o による 25 MeV 中性子の検出が理論の証拠となる。

（3）発熱量の増大：^{7}Li を追加することで軽水素炉の発熱量が増大すると推定しており、実証が必要。

（4）連続運転条件の確立：重水素炉では ^{6}Li が再生成されるため、D2 ガス供給のみで長期連続運転が可能と考えられる。適切な D_2 供給速度の最適化が課題である。

7. まとめ

(1) 75° C において Pd/^{6}Li 系で α 線源起動により、軽水素炉（1.5 時間連続 γ 線放出）と

重水素炉（最大 52.4 μSv/h・中性子爆発）の起動を確認した。連鎖増幅なしで推定したγ線発生率（約 3×10^{-18} s^{-1}）と観測値（約 3×10^{5} s^{-1}）との差は 22 桁に達し、連鎖反応の成立を定量的に示す。

(2) 「死後の熱」の起点は熱中性子と ^{6}Li の核反応であり、高 D 濃度は必要ではない。Pd-H 状態図の解析から、「死後の熱」は D 濃度の低いα相で起きており、高 D 濃度が有利とする Pons らの推定はミスリードであった。

(3) Kasagi ら・Uneme らの実験による異常粒子（17.2 MeV 以下の p、6.7MeV 以下の α 等）は、DD binary を中間状態とする DDD3 体核融合反応（式 i〜k）で説明でき、各粒子エネルギーはエネルギー保存則（Q 値）と一致する。

(4) 通常の DD 核融合反応（式 d〜h）では^{6}Li は生成されない。Okamoto らの SIMS データにおける^{6}Li/^{7}Li 比変化（7.5:92.5→1:1）を説明できる核反応経路は、本論文が提案する DDD3 連星核への D 核衝突反応（式 l）のみである。

(5) 観測された中性子バーストの周期的発生（表 1）は、長距離核力（$-NA/r^4$）[9]に基づく DD 連星核・DDD3 連星核の蓄積期と、その連鎖的崩壊による爆発期・回復期の 3 段階モデルで説明できる。本モデルを提案する。

(6) 軽水素金属格子型核融合炉は放射線が少なく、重水素炉では式(l)による^{6}Li の再生成が起きるため D_2 ガス供給のみで長期連続運転が原理的に可能と予測される。本原理に基づく金属格子型核融合炉の実現を目指す。

参考文献

[1] M. Fleischmann and S. Pons, "Calorimetry of the Pd-D2O system," Phys. Lett. A 176, 118 (1993).

[2] O. Iwamoto et al., "JENDL-5," Japan Atomic Energy Agency (2021).

[3] S. Uneme, "Studies of nuclear reactions in solid in TiDx ," JCF2-20.

[4] J. Kasagi et al., "Energetic protons and α particles emitted in 150-keV deuteron bombardment on deuterated Ti," J. Phys. Soc. Japan 64(3), 777 (1995).

[5] M. Nakada, T. Kusunoki, M. Okamoto, O. Odawara, "A Role of Lithium for the Neutron Emission in Heavy Water Electrolysis," Third International Conference on Cold Fusion, Universal Academy Press, Tokyo, 1993.

[6] 大山和男, JCF23 Proceedings (2023).

[7] 大山和男, JCF24 Proceedings (2024)

[8] Martin Fleischmann and Stanley Pons in: Frontiers of Cold Fusion: Proceedings of the Third International Conference on Cold Fusion, Nagoya, Japan (21-25 October 1992), ed. H. Ikegami, Frontiers Science Series No. 4 (FSS-4) p.47.

[9] K. Ooyama, "A long-range r-4 nuclear potential as the origin of the 1/v law and energy-independent

elastic scattering in light nuclides" Research Square preprint, https://doi.org/10.21203/rs.3.rs-9630167/v1 (2026).

[10] Kwon JU, Kim JC, Chung HI. Cross sections for the 6Li(p,3He)4He reaction. Nucl Phys A. 1989;493(1):112–120. (EXFOR entry F0062.003)

[11] Bashkin S, Richards HT. Reaction of protons with Li6. Phys Rev. 1955;97(5):1245–1249. (EXFOR entry C1588.003)

[12] K. Ooyama, "Observation of Anomalous Gamma-Ray and Neutron Emissions from 6Li-doped Palladium under Hydrogen and Deuterium Loading" Research Square preprint, https://doi.org/10.21203/rs.3.rs-10086889/v1 (2026).

A note without reviewing

Mechanism of CF I: Fusion induced by dislocation annihilation

S. Fukuta
email: luckfield29@gmail.com

June 24, 2026
(first submitted: April 2, 2026)

Abstract

To explain cold fusion in the palladium–deuterium system, we propose a fusion model induced by dislocation annihilation. Through atomic-scale confinement induced by both macroscopic forces accompanying dislocation annihilation and a quarter-electron electrostatic shielding (QEESS), ^{4}He-like fusion precursors are formed. This confinement enables static nuclear fusion, leading to the selective production of thermodynamically the most stable ^{4}He.

This model demonstrates that the cold fusion in palladium-deuterium systems corresponds to a miniature of pycnonuclear fusion, occurring in white dwarfs and neutron stars. In this sense, the LENR reactor is a real-world version of the "degenerate reactor" often depicted in science fiction literatures, built of ordinary matters.

From this model, various properties — such as the (D/Pd) loading effect, the influence of dislocation density and nuclear transmutation — can be derived not only qualitatively but also quantitatively.

Finally, Paneth's experimental results from the 1920s were reevaluated. The amount of helium predicted by our model suggests that it is highly likely that their results were correct as the earliest proof for cold fusion.

Keywords: Fleischmann-Pons effect, cold fusion, solid-state nuclear fusion, Huizenga's three miracles, dislocation, D-D fusion, palladium, helium, deuterium, deuteron, transmutation, Hagelstein, McKubre, Miles, Storms, Iwamura, Szpak, Paneth, dislocation annihilation, atomic-scale confinement, quarter-electron electrostatic shielding, fusion precursor, pycnonuclear fusion, LENR

1 Introduction

In the development of civilization, it is desirable for energy costs per unit to decrease at a rate less than inversely proportional to energy consumption from the perspective of economic rationality. Figure 1 shows the global energy consumption trend from 1820 to 2020 over 200 years and the estimated energy costs per kWh, respectively. During the 19th century, energy costs per unit fell more than energy consumption increased, allowing civilization to maximize its potential without worrying about the cost burden of energy. In contrast, the 20th century saw energy costs rise after the 1973 oil crisis, forcing civilization to develop while enduring the burden of energy costs.

If low energy cost per unit below 1 cent/kWh can be achieved, 21st-century civilization will once again unleash its inherent potential. Consequently, global problems including food starvation will be resolved. One of the most promising candidates for such a low-cost clean energy source is the cold fusion reactor, which is expected to provide an inexhaustible supply of fuel.

Since the historic announcement by Fleischmann and Pons in 1989[2], cold fusion has been dismissed with skepticism, despite the existence of clear experimental evidences of nuclear reactions from the early beginning[3, 4]. As a result of the improvement of both the reproducibility and performance of cold fusion, the U.S. government has begun allocating funds to cold fusion researches, and DARPA has launched the MARRS program[5] since 2025-12-31. This program aims to develop quantitative models based on specific mechanisms and to create scalable, distributed energy sources within a few years.

To explain cold fusion in the palladium–deuterium system, we propose a fusion model induced by dislocation annihilation[6]. For simplicity, the dissipation of mass-deficit energy and tritium production[7] are omitted. However, this type of fusion can be explained both qualitatively and quantitatively, including the (D/Pd) loading effect[8] in the Fleischmann-Pons effect.

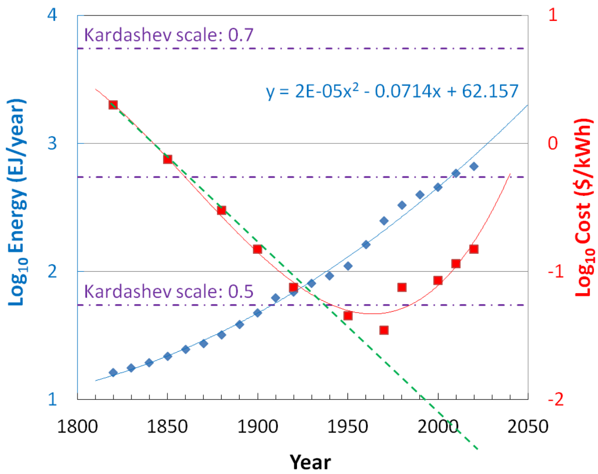

Figure 1: Historical trends in global primary energy consumption and energy cost per kWh1.

2 Fundamental concepts and mechanism of D-D nuclear fusion induced by dislocation-annihilation

In the cold fusion in palladium-deuterium systems, ^{4}He production dominates over ^{3}He and T productions. Moreover, a strong correlation between ^{4}He yield and excess heat was confirmed by Miles[9], McKubre and Hagelstein[10]. Although the domination of ^{4}He production cannot occur in the dynamic nuclei collisions with short reacting time, it can be enabled by static or quasi-static reactions with extremely long reacting time. In static reactions, the equilibrium state becomes dominant. The stabilization energies for T, ^{3}He and ^{4}He are 4.04 MeV, 3.27 MeV, and 23.9 MeV, respectively, leading to a complete transition to ^{4}He. Therefore, examining both the Fleischmann-Pons effect and the physical properties of palladium, we conclude that the static D-D fusion occurs due to dislocation annihilation.

Muon-catalyzed fusion is also classified as cold fusion. Although the distance between deuterons is reduced to approximately 500 fm by muons, leading to fusion via the tunneling effect, the production channels are nearly identical with those of thermonuclear D-D fusion, and almost no ^{4}He is produced. Therefore, since it is considered that in the palladium-deuterium systems, the distance between deuterons must be reduced to the order of the nuclear size, ranging from 1 fm to 50 fm.

Figure 2 illustrates the concept of the dislocation-induced fusion. When a dislocation exists, excess deuterium atoms are adsorbed onto the palladium atoms at the dislocation. When the dislocation disappears due to crystalline recovery from external excitation such as heat, two deuterium atoms are forcibly pushed into one hydrogen-storage site. This atomic-scale confinement leads to quasi-static nuclear fusion among nuclei with low kinetic energy. This model concretizes either the nuclear fusion mechanism proposed by Arata[11] or Nuclear-Active-Environment (NAE) by Storms[12]. Moreover, although nuclear fusion induced by dislocation annihilation has already been proposed by Ooyama[13], dynamic fusion by collision of nuclei is assumed.

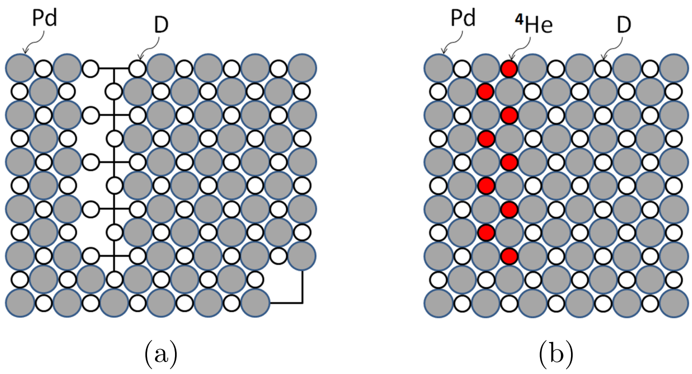

Figure 2: Concept images of D-D fusion induced by annihilation of dislocation; (a)a lattice with dislocation, where excess deuterium atoms are adsorbed on palladium atoms, (b)the lattice after annihilation of dislocation to produce ^{4}He atoms.

The dislocation energy density u_{dis} in palladium is estimated to be approximately 20 MJ/m^3 under conditions of extremely high dislocation density ($\rho = 1 \times 10^{16}/\mathrm{m}^2$) resulting from cold working [14]. ρ represents the total length of dislocation lines per unit volume of a palladium crystal. Applying a lattice constant $a \simeq 4 \times 10^{-10}$ m, the energy per dislocation site ϵ_{dis} of palladium is estimated to be

$$\epsilon_{dis} \simeq u_{dis} a/\rho \simeq 8 \times 10^{-19}\mathrm{J/site} \simeq 5\mathrm{eV/site}. \quad (1)$$

This value is comparable to the eigenenergy values of a hydrogen atom. Therefore, it is completely impossible to bring deuterons into close proximity to a distance equal to their nuclear size of the order of 1 fm, concluding that some form of effective electrostatic screening is necessary. However, the effect of Thomas-Fermi screening, which has been frequently applied to cold fusion theories, is so weak as to be negligible. Therefore, we propose the quarter-electron electrostatic shielding (QEESS) shown in Figure 3. With this configuration, the forces acting on the two deuterons and the quarter electron cancel each other to become zero, achieving complete electrostatic screening. The density function $\rho(\mathbf{r})$ of two electrons of deuterium atoms is approximately given by

$$\rho(\mathbf{r}) \simeq \frac{1}{4}\delta - like(\mathbf{r}) + \frac{7}{4}\phi_0^*(\mathbf{r})\phi_0(\mathbf{r}), \quad (2)$$

where $\phi_0(\mathbf{r})$ is a basis function of an electron. Since the quarter electron is not a perfect delta function, it is preferable for it to be spread out as much as possible between the two deuterons, as this minimizes the formation energy. This is a type of cooperative quantum phenomenon that arises from a large number of eigenfunctions, such as Bose-Einstein condensation. It is considered that cold fusion is temperature-insensitive due to the quantum effect associated with a single electron. Therefore, while the ground-state energy can be determined using density functional theory (DFT), the upper limit energy for the formation of a quarter electron is estimated to be $0.25|E_1| \simeq 0.25 \times 13.6\text{eV} = 3.4\text{eV}$. Here, $|E_1|$ is the Rydberg unit of energy, which is the ionization energy of an electron in the ground state of a deuterium (hydrogen) atom. This formation energy is smaller than the dislocation energy given by Equation (1), indicating that it is entirely feasible via dislocation annihilation.

Approximating an quarter electron as a point charge in Figure 3, the Coulomb force F experienced by the deuteron, changing the distance r to the quarter-electron, is given by

$$F = \frac{e^2(3r + r_0)(r - r_0)}{4 \cdot 4\pi\epsilon_0 \cdot r^2(r + r_0)^2} = \frac{e^2}{4 \cdot 4\pi\epsilon_0 r_0^2} \cdot \frac{(3x + 1)(x - 1)}{x^2(x + 1)^2}, \tag{3}$$

where $x = r/r_0$. Figure 4 shows the dependence of the normalized Coulomb force F on the normalized distance x, with the coefficients $(e^2/4 \cdot 4\pi\epsilon_0 r_0^2)$ in Equation 3 removed. This clearly indicates that this state is unstable. However, QEESS is considered to escape the destruction by the compressive force resulting from dislocation annihilation.

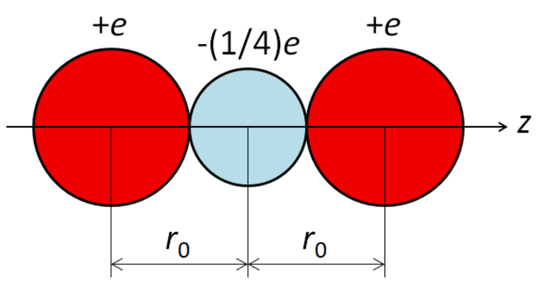

Figure 3: Quarter-electron electrostatic shielding to cancel the repulsion between two deuterons.

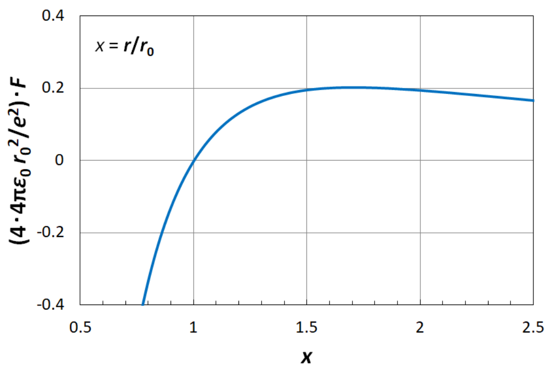

Figure 4: Coulomb force of the deuteron changing the distance to a 1/4 electron.

Figure 5 shows the energy levels during the process leading to dislocation annihilation fusion. The ground-state energies of isolated deuterium atoms and a deuterium molecule are -27.2 eV and -32.0 eV, respectively. In a hydrogen (deuterium) molecule, electrostatic screening occurs due to approximately 0.3 electrons. While the instability caused by the progression of dislocation annihilation is stabilized by lowering the energy through localized-electron electrostatic screening, QEESS is considered to achieve this with the minimum necessary energy. A ^{4}He-like fusion precursor realized by QEESS corresponds to an atom with atomic number $Z = 1.75$, so its energy level is close to that of helium, -78.9 eV. A rough estimate gives ground-state energy of $-78.9 * (Z/2)^2 = -60.4\text{eV}$, multiplied by the electron fraction $(1.75/2)$, resulting in -52.9 eV. More precisely, applying the perturbation method [15], the ground-state energy E of two electrons in an atom of atomic number Z is given by $E = -\{Z^2 - (5/8)Z)\} \cdot 2|E_1|$. Here, since Z is smaller than two, incorporating this correction, the ground-state energy E is estimated to be

$$E = -\left(Z^2 - \frac{5}{8}Z\right) \cdot Z|E_1|. \tag{4}$$

Substituting $Z = 1.75$ yields $E = -46.9\text{eV}$. Here, the formation energy of the QEESS is estimated to be $46.9 \cdot (0.25/1.75) = 6.69\text{eV}$ at most. Thus, through dislocation annihilation, the two deuterons are transformed into a ^{4}He-like fusion precursor that is approximately 19.7 eV more thermally stable than the initial state, ultimately enabling the selective production of ^{4}He by static nuclear fusion.

Figure 6 shows the evolution of the ground-state energy as the inter-deuteron distance $2r$ decreases to zero due to dislocation annihilation. Denoting the Bohr radius by a_0, the value of $(2r/a_0)$ ranges from 2 to 1.4, and two isolated deuterium atoms transform into a deuterium molecule. In quantum chemistry, the electrostatic screening electrons between the two deuterons are estimated to be 0.3 electrons, and the repulsion between the two nuclei is eliminated. Since the deuterium molecule is a stable state in deuterium-system, $(2r/a_0)$ is reduced by the compressive stress accompanying dislocation annihilation, building resilience with the decrease of electrostatic screening due to inter-nuclear electrons. When the electrostatic shielding electrons fall below 0.25, localized-electron electrostatic shielding forms as a relaxation mechanism. At this point, if the inter-nuclear distance becomes sufficiently short, QEESS forms, allowing the two deuterium nuclei to be treated as a single entity, causing the energy level to drop sharply; consequently, the inter-nuclear distance automatically decreases, and a ^{4}He-like fusion precursor is formed. At this point, a central force arises in the nucleus due to central symmetry, and at distances on the order of 1 fm, the Yukawa potential arises due to meson exchange; therefore, it is considered that the inter-nuclear distance could potentially be reduced to less than 1 fm. Consequently, thermally stable ^{4}He is formed through static fusion. During dislocation annihilation, the energy of the deuterium system immediately drops by approximately 4.74 eV due to deuterium molecule formation and ultimately falls to -46.9 eV; therefore, it is considered impossible for a deuterium atom to escape to the T-site.

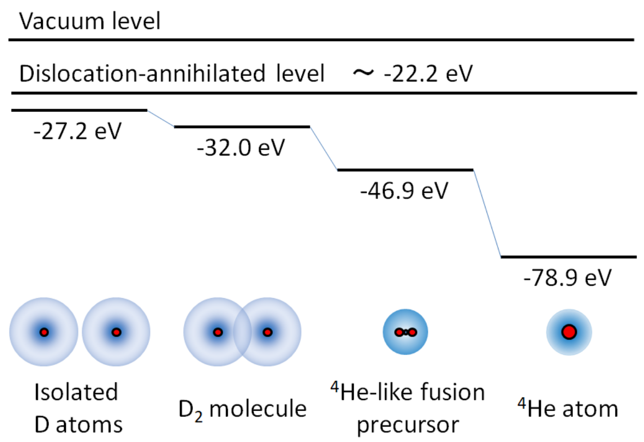

Figure 5: Energy levels of two deuterium atoms in processes inducing dislocation-annihilation fusion.

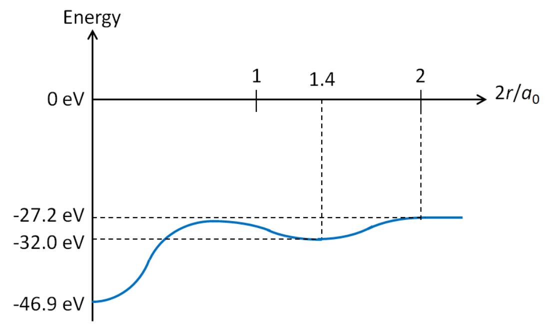

Figure 6: Rough image of the dependence of energy on the distance between deuterons.

If both nuclei are protons, the ^{2}He-like fusion precursor ($Z = 1.75$) formed by dislocation annihilation is considered to exist as a stable state without fusion occurring, since it contains no neutron. This is significant because it could serve as direct evidence for the existence of the fusion precursor. Since the binding energy of protons and neutrons in a deuteron is 2.22 MeV, the nuclear binding energy of the ^{2}He-like molecule appears to be in the range of 1 keV to 100 keV if the distance between them is sufficiently close. Therefore, it is entirely possible that the the ^{2}He-like molecule is stable and will not decay under excitation of less than 1 keV, and verification via optical transitions of electrons may be possible. Furthermore, since this molecule exhibits characteristics of degenerate matter found in white dwarfs and neutron stars, it is also important in astrophysics.

Furthermore, since this molecule has the same mass number as ^{2}He, its thermal velocity is $\sqrt{2}$ times that of ^{4}He, and thus its thermal conductivity is approximately $\sqrt{2}$ times larger. The critical temperature for superfluidity is also doubled. Consequently, there are high expectations for its application as a coolant with performance exceeding that of ^{4}He.

However, if an excitation energy of 0.782 MeV or greater realizes the transformation of a proton into a neutron via the '*weak*' interaction, the following nuclear reaction

$$\mathrm{H} + \mathrm{H} \longrightarrow \mathrm{D}(E_D) + \nu_e(E_\nu), \quad \text{where } E_D + E_\nu = 1.442 \text{ MeV}, \tag{5}$$

is possible. Therefore, if this reaction probability is sufficiently high, the ^{2}He-like fusion precursors will be consumed and disappear.

Thus, dislocation-annihilation fusion is a form of fusion that replicates the principle of pycnonuclear fusion — which occurs in high-density stars such as white dwarfs and neutron stars — at defect sites within a solid; it is fundamentally different from plasma confinement fusion, which replicates the principle of thermonuclear fusion in the Sun. This fusion reactor is the real-world equivalent of a "degenerate reactor" from science fiction.

In dislocation-annihilation fusion, Huizenga's three miracles are achieved as follows:

- Through atomic-scale confinement induced by both macroscopic forces accompanying dislocation annihilation and a quarter-electron electrostatic shielding (QEESS), ^{4}He-like fusion precursors are formed. This confinement enables static nuclear fusion, leading to the selective production of thermodynamically the most stable ^{4}He.
- No neutron is essentially produced due to the selective ^{4}He production.
- The spin-orbit coupling term symbol for the ground state of a deuteron is $^3\mathrm{S}_1$, and the term symbol for the nucleus synthesized by nuclear fusion is $^3\mathrm{S}_1 \times {}^3\mathrm{S}_1 = {}^1\mathrm{S}_0 + {}^3\mathrm{S}_1 + {}^5\mathrm{S}_2$. The term symbol for the ground state of the doubly magic nucleus ^{4}He is $^1\mathrm{S}_0$. According to the optical transition rule, photon emission such as gamma rays via both E1 and M1 transitions is forbidden; therefore, the mass defect energy is ultimately dissipated as heat through alternative pathways. It is considered that processes such as neutron production, which occur on the MeV scale, play a significant role [7].

From this model, various properties can be derived both qualitatively and quantitatively. The subsequent sections will discuss (D/Pd) loading effect, dislocation density, nuclear transmutation and Paneth's reevaluation, respectively.

3 Influence of (D/Pd) loading

We determine the dependence of dislocation-annihilation fusion on (D/Pd) loading. Figure 7 shows the crystal structure of PdD. The crystal center is defined as the dislocation annihilation point. For fusion to occur, 2 deuterium atoms are required, and furthermore, all 12 neighboring O-sites must be fully occupied by deuterium atoms so that the deuterium atoms at the center cannot escape. As discussed in the previous section, the central pair of deuterium atoms is expected to fuse certainly through dislocation annihilation. Therefore, the fusion probability P_f is given by

$$P_f = \left(\frac{D}{Pd}\right)^{14}. \tag{6}$$

Figure 8 shows the dependence of P_f on (D/Pd). Since dislocation annihilation occurs due to macroscopic forces such as stress, dislocations of a certain length are annihilated all at once. This corresponds to the mini-explosions of hot spots observed by Szpak[16], and the noisy behavior of the excess heat is consistent with this model. Therefore, it is appropriate to set the fusion probability at which excess heat is observed to $P_f = 0.1$, and the threshold $(D/Pd)_{th}$ is estimated as

$$\left(\frac{D}{Pd}\right)_{th} = 0.1^{(1/14)} = 0.848 \simeq 0.85. \tag{7}$$

This value is fortuitously consistent with the thresholds reported by McKubre[8].

Well-known experimental data of excess heat dependence on (D/Pd) loading in Pd-D systems by McKubre[8] are shown in Figure 9 (a), and the analyzed results in Figure 9 (b). As the exponent of (D/Pd) is ranging from 14 to some extent, other parameters such as current density, dislocation density and temperature must likely be taken into account.

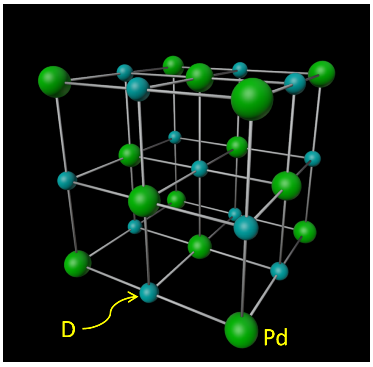

Figure 7: 3D ball-and-stick image of a PdD crystal.

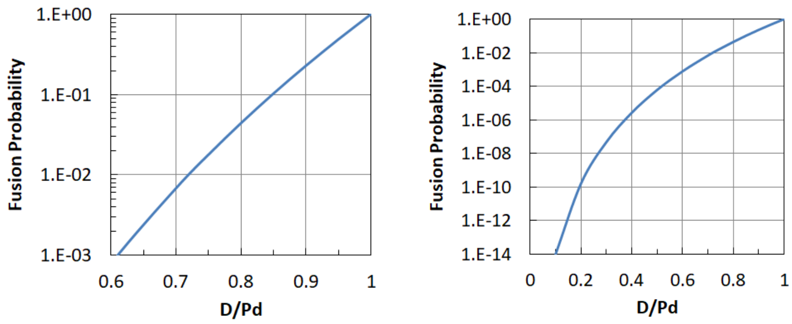

(a) (b)

Figure 8:
Dependence of probability of dislocation-annihilation fusion on (D/Pd) loading (a) and the enlarged graph (b).

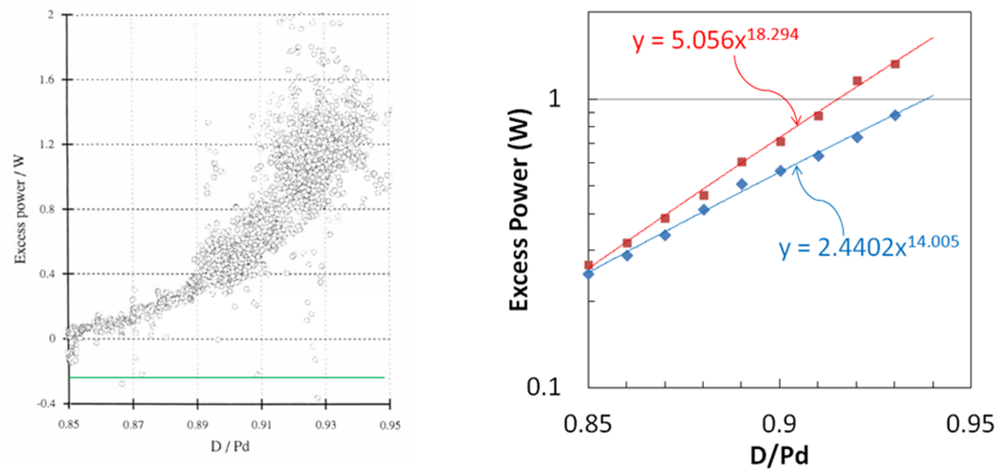

(a) (b)

Figure 9: Dependence of excess heat generation on (D/Pd) loading. (a)Measurement data reproduced from McKubre[8]. A green line at -0.249 W of excess power is new zero level. (b)Analyzed results of data (a). Blue and red points represent the lower limits and median values of the measurement data, respectively.

4 Influence of dislocation density

Miles[9] demonstrated that the excess heat generation in Pd-D systems exhibits strong manufacturer dependence. This is also considered to be due to the influence of dislocations. Specifically, manufacturing processes such as rolling and heat treatment differ by manufacturer, resulting in significantly varying dislocation densities. While the dislocation density of general metals including palladium is increased to a range from $10^{14} - 10^{16}/\mathrm{m}^2$ by cold working, it is reduced to a range from $10^{11} - 10^{13}/\mathrm{m}^2$ by annealing. Miles[9] reported manufacturer dependence in excess heat generation, which ranged from 0 to 15 MJ/cc. Table 1 summarizes the highest excess heat generation density calculated from Miles. Palladium supplied from Johnson Matthey plc had the best performance, and that of NRL the second best.

Table 1: Excess heat generation densities, calculated from Miles[9].

Cathode model	d (mm)	V (cc)	Excess heat (kJ)	Heat density (MJ/cc)	Year	Days
Johnson Matthey Pd	6.35	0.36	210	0.583	1989	26
Johnson Matthey Pd	6.35	0.36	220	0.611	1989	26
Johnson Matthey Pd	6.35	0.36	300	0.833	1989	38
Johnson Matthey Pd	6.35	0.36	1400	3.889	1990	83
Johnson Matthey Pd	1	0.02	290	14.5	1992	66
NRL PdB (0.75%)	6	0.57	950	1.667	1994	137

If the dislocation density is denoted by ρ ($/\mathrm{m}^2$) and the lattice constant by $a = 3.8907$ Å, the dislocation site density can be estimated as ρ/a (sites/m^3). Multiplying this by the fusion probability P_f, given by Equation (6), and the mass defect energy of a single ^{4}He nucleus (23.8 MeV) yields the excess heat generation density per unit volume, q_{eh}, which is estimated as

$$q_{eh} \simeq \left(\frac{\rho}{a}\right) \cdot 23.8 \cdot \left(\frac{D}{Pd}\right)^{14} \ (\mathrm{MeV/m^3}) = 9.80 \times 10^{-9} \cdot \rho \left(\frac{D}{Pd}\right)^{14} \ (\mathrm{J/cc}). \tag{8}$$

Generally, it is reasonable to assume that the condition $0.1 \le (D/Pd)^{14} \le 1$ was satisfied. For the maximum excess heat generation density of 14.5 MJ/cc shown in Table 1, $1.48 \times 10^{15}\ /\mathrm{m}^2 \le \rho \le 1.48 \times 10^{16}\ /\mathrm{m}^2$ is estimated; this estimation includes the upper limit of dislocation density due to cold working, suggesting that his experiments, including the material selection, were likely excellent.

5 Nuclear transmutation

Dislocation-annihilation fusion can also explain nuclear transmutation. In the well-known transmutation experiments by Iwamura[17], a given nucleus fuses with a specific number of deuterium nuclei (such as 2, 4, or 6) to selectively transform into a specific nucleus. Figure 10 illustrates the mechanism of nuclear transmutation via dislocation annihilation. The annihilation transmutes a complex ion into a specific nucleus at the dislocation. The typical coordination number of a complex ion is 2, 4 or 6, which seems consistent with the experimental results.

The conditions for complete localized-electron electrostatic shielding with respect to complex ions are far more difficult than the QEESS valid for the two identically charged nuclei shown in Figure 3, and have not yet been investigated. As a simple example, Figure 11 illustrates the localized electron electrostatic shielding for both a deuteron and a nucleus with charge $+Ze$. Solving the system of equations for the Coulomb force, assuming the charge of the localized electron between the nuclei is $-\kappa e$, κ is given by

$$\kappa = \frac{Z}{(1+\sqrt{Z})^2}. \tag{9}$$

Figure 12 shows the dependence of κ on Z. In the limit as $Z \to \infty$, $\kappa \to 1$. However, the convergence is quite slow. For $Z = 1$, 8, 50, and 100, κ is 0.25, 0.546, 0.768, and 0.826, respectively.

The transmutation into Mg, Al, Si, Ca, and Zn was observed by Szpak[18] via Pd-D codeposition from a 0.3 M LiCl heavy water solution. As shown in Table 2, this can be explained by nuclear transmutation from oxygen, the main atom of the aqueous solution except deuterium. Identifying the origin of Zn is difficult and remains a challenge for future research. The nuclear transmutation demonstrated by Miley[19] is considered to be the result of multiply repeated ones from oxygen.

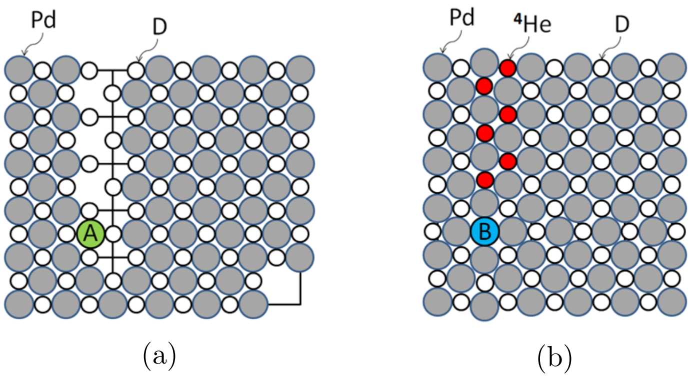

Figure 10: Concept images of transmutation by dislocation-annihilation fusion; (a)an ion A segregates to dislocation, forming an complex ion [A D_n], (b)an ion B is transmuted from the complex ion [A D_n] by nuclear fusion.

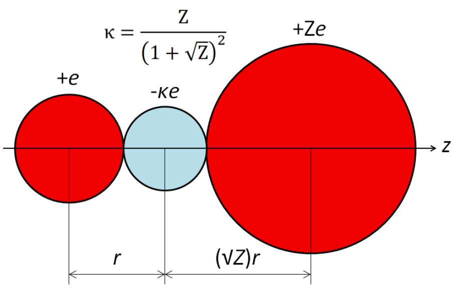

Figure 11: Localized-electron electrostatic shielding between $+e$ and $+Ze$ nuclei.

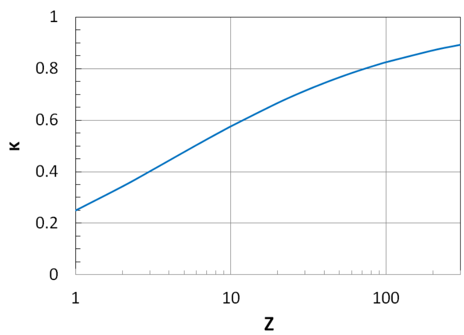

Figure 12: Dependence of the charge ratio of localized electron on atomic number Z.

Table 2: Transmutation at a blister in Pd-D codeposit by Szpak[18]

$^{16}_{8}O + 4\,D \longrightarrow\ ^{24}_{12}Mg$,	$^{16}_{8}O + 6\,D \longrightarrow\ ^{28}_{14}Si$,	$^{28}_{14}Si + 6\,D \longrightarrow\ ^{40}_{20}Ca$
$^{16}_{8}O + (5\,D + H) \longrightarrow\ ^{27}_{14}Si\,(T_{1/2} = 4.111\,s) \longrightarrow\ ^{27}_{13}Al$		
$^{40}_{20}Ca + 6\,D \longrightarrow (^{52}_{26}Fe)\,(T_{1/2} = 8.275\,h)$, $(^{52}_{26}Fe) + 6\,D \longrightarrow (^{64}_{32}Ge) \longrightarrow\ ^{64}_{30}Zn$?		
$[^{(6,7)}_{3}Li^{+}\,(OD)^{-}\ ^{(35,37)}_{17}Cl^{-}\ D^{+}] \longrightarrow\ ^{(61,62,63,64)}_{30}Zn$?		

6 Reevaluation of Paneth

Sixty years before the historic announcement of Fleischmann and Pons[2], Paneth *et al.*[20, 21] reported nuclear transmutation from hydrogen to helium in 1926, but retracted it the next year[22, 23]. As their work is historically innovative and significant, We do reevaluate it.

Summarizing the researches by Paneth *et al.*[20, 21]:

- Since deuterium had not yet been known before the discovery in 1931, they must have experimented using light hydrogen (protium) containing deuterium at its natural abundance ratio of 1.15×10^{-4}.
- To produce helium more efficiently, sponge palladium, palladium black and palladinized asbestos were used. From a modern perspective, these materials are nanoparticles, which have not only the largest specific surface area to promote hydrogen absorption but also the highest dislocation densities to promote cold fusion.
- From sponge palladium or palladium black, helium volume ranged from the detection limit of 10^{-9} cc to 10^{-8} cc was obtained.
- From 1 g of 50% palladinized asbestos, on the order of 10^{-6} cc of helium was obtained. Since palladinized asbestos was formed by electroless plating, it is not surprising that it has the particularly highest dislocation density near the theoretical limit of on the order of 10^{18} /m^2.
- The palladium activity to produce helium gradually decreased and became lost in repeated experiments. The activity could be refreshed by heating. This can be interpreted as meaning that dislocations were consumed for fusion during experiments, and edge dislocations were reintroduced during cooling after heating due to thermal stresses occurring between the surface and interior.

These behaviors seem quite reasonable from our model. However, Paneth retracted the transmutation of hydrogen into helium by palladium, because he noticed 10^{-9} cc of helium penetration through glass tubes from the air and initial helium absorption in the asbestos[22, 23]. Initially, he retracted only the results concerning the palladinized asbestos, maintaining that the experimental data for sponge palladium and palladium black remained valid. However, he ultimately retracted the all results, citing the possibility of "unknown" errors. This was not a complete denial but a passive retraction. Based on current knowledge, it seems entirely possible that they succeeded in the transmutation of hydrogen into helium.

It is possible to estimate their helium yield using our model. In the fusion of protium nuclei with deuterium at its natural abundance ratio of 1.15×10^{-4}, the ^{4}He produced from two deuterium nuclei can be neglected, and only ^{3}He from both hydrogen and deuterium has to be considered. From

Equation (8) with the abundance ratio of deuterium[6], the ^{3}He volume V_{He3} (cc) under standard conditions is given by

$$V_{He3} \simeq 1.779 \times 10^{-18} M\rho \left(\frac{H}{Pd}\right)^{14}, \tag{10}$$

where M and ρ represent the sample weight (kg) and dislocation density (/m^2), respectively. (H/Pd) loading is approximately 0.65 at room temperature and 1 atm hydrogen pressure. The current standard state for a gas is defined as the condition at 0 °C under 0.1 MPa pressure. On the other hand, in the 1920s, it was approximately defined as that at room temperature under the pressure at 1 atm = 0.101325 MPa. Therefore, although the values from the 1920s are nearly the same, they are considered to be 5–6 % higher than modern values.

For sponge palladium or palladium black, using M = 1 g = 10^{-3} kg and $\rho = 10^{15}/\text{m}^2$, equation (4) yields $V_{He3} = 4.275 \times 10^{-9}$ cc. This dislocation density corresponds to reported values for nano-particle palladium. For 1 g of 50% palladinized asbestos, using $\rho = 10^{18}/\text{m}^2$, $V_{He3} = 2.138 \times 10^{-6}$ cc is obtained. These values agree remarkably well with Paneth's experimental data, suggesting that their experiments were likely correct and warrant reevaluation.

Assuming that ^{2}He-like fusion precursors fuse completely to form deuterons, the number of deuterons produced is estimated to be $(H/2D) \simeq 4,348$ times the number of ^{3}He nuclei produced simultaneously. When $V_{He3} = 10^{-8}$ cc, the mass defect energy is approximately 270 J. Given that the heat capacity of palladium at 25 °C is 25.98J/(mol · K) $\simeq$ 0.244J/(g · K), this energy would cause 1 g of palladium to heat up by approximately 1100 °C. Since palladinized asbestos generated 100 times this amount of energy, it is considered that the ^{2}He-like precursors remained largely unfused. On the other hand, there are reports of excess heat generation involving protium and metals. Since there may be conditions that cause differences between the two, further research will be needed.

7 Conclusions

To explain cold fusion in the palladium-deuterium system, known as the Fleischmann–Pons effect, We proposed a fusion model induced by dislocation annihilation. Through atomic-scale confinement induced by both macroscopic forces accompanying dislocation annihilation and a quarter-electron electrostatic shielding (QEESS), ^{4}He-like fusion precursors are formed. This confinement enables static nuclear fusion, leading to the selective production of thermodynamically the most stable ^{4}He.

This model demonstrates that the cold fusion in palladium-deuterium systems corresponds to a miniature of pycnonuclear fusion, occurring in white dwarfs and neutron stars. In this sense, the LENR reactor is a real-world version of the "degenerate reactor" often depicted in science fiction literatures, built of ordinary matters.

From this model, the reaction probability and excess heat generation are derived to be proportional to $(D/Pd)^{14}$. The threshold deuterium loading ratio required for excess heat generation is calculated as $0.1^{(1/14)} \simeq 0.85$, fortuitously consistent with McKubre's law. The model also explains the dependence of excess heat generation on material properties across different manufacturers and predicts a maximum heat generation density close to values estimated from dislocation density.

Nuclear transmutation is considered to be fused in a single step from the complex ion segregating at dislocation by the annihilation. This may be the reason why a certain nucleus fuses with a fixed number of deuterons. This model also unifies Iwamura's nuclear transmutation from heavy metal nuclei with that from oxygen nuclei in palladium-heavy water systems.

Finally, Paneth's experimental results from the 1920s were reevaluated. When the amount of helium predicted by our model was estimated, it showed remarkable agreement with their reported values, suggesting that Paneth's experimental observations were likely correct as the earliest excellent proof for cold fusion.

References

[1] S. Fukuta, "Relationship between energy consumption and cost in civilization development", Zenodo,2026. Available at: https://doi.org/10.5281/zenodo.18358290

[2] M. Fleischmann and S. Pons, *J. Electroanal.Chem.*, **261**, pp.301-308 (1989).

[3] E. Yamaguchi and T. Nishioka, *Japan J. Appl. Pys.*, **29**, pp.L666-L669 (1990).

[4] P. K. Iyengar and M. Srinivasan, *Proc. of ICCF-1*, pp.62-81 (1990).

[5] DARPA, "MARRS: Mechanisms for Amplification of fusion Reaction Rates in Solids", 2025-12-31. Washington DC: U. S. Department of Defense.
Available at: https://www.darpa.mil/research/programs/marrs-mechanisms-amplification-fusion-reaction-rates-solids

[6] S. Fukuta, "Mechanism of cold fusion I: Nuclear fusion induced by dislocation annihilation", Zenodo,2026. Available at: https://doi.org/10.5281/zenodo.18266917

[7] S. Fukuta, "Mechanism of cold fusion II: Energy dissipation and neutron production", Zenodo,2026. Available at: https://doi.org/10.5281/zenodo.19292807

[8] M. C. McKubre *et al.*, *Proc. ICCF-3*, **1**, pp.5-19(1992).

[9] M. H. Miles *et al.*, Final Report, NAWCWPNS Technical Publication 8302, Naval Air Warfare Center Weapons Division (1996).

[10] P. L. Hagelstein *et al.*, *Proc. ICCF-11*, pp.23-59 (2006).

[11] Y. Arata *et al.*, *Proc. Jpn. Acad., Ser. B*, **78**, pp.201-204 (2002).

[12] E. Storms, *J. literatures Matter Nucl. Sci.*, **20**, pp.100-138 (2016).

[13] K. Ooyama, *Proc. JCF18*, p.55 (2017). Available at: https://jcfrs.org/file/jcf18-proceedings.pdf

[14] D. J. Nagel and M. A. Imam, *Proc. ICCF-10* (2003).
Available at: https://lenr-canr.org/acrobat/NagelDJenergetics.pdf

[15] L. D. Landau and E. M. Lifshitz, "*Quantum Mechanis: Non-Relativistic Theory*", Butterworth-Heinemann, Chap. 10 (1981).

[16] S. Szpak *et al.*, *Proc. ICCF-10* (2003).
Available at: https://lenr-canr.org/acrobat/SzpakSpolarizedd.pdf

[17] Y. Iwamura *et al.*, *J. Condensed Matter Nucl. Sci.*, **10**, pp.63-71 (2013).

[18] S. Szpak *et al.*, *Proc. ICCF-11* (2006).
Available at: https://lenr-canr.org/acrobat/SzpakSprecursors.pdf

[19] G. H. Miley *et al.*, *J. New Energy*, **1**(3), pp.5-30 (1996).

[20] F. Paneth *et al.*, *Berichte der Deutchen Chemischen Gesellschaft(Ber. Dtsch. Chem. Ges.)*, **59**, pp.2039-2048 (1926). Available at: https://lenr-canr.org/acrobat/PanethFthepublica.pdf

[21] *Nature(London)*, **118**, pp.526-527 (1926).

[22] F. Paneth, *Nature(London)*, **119**, p.706 (1927).

[23] F. Paneth, K. Peters and P. Günther, *Ber. Dtsch. Chem. Ges.*, **60**, pp.808-809 (1927).